Published OnlineFirst March 3, 2011; DOI:10.1158/1078-0432.CCR-10-2638

Table 2. Summary of AEs (≥20% all grades, all cycles; $n = 27$)

AEs	Patients, *n* (%)				
	Grade 1	Grade 2	Grade 3	Grade 4	Total
Hematuria	20 (74.1)	0	0	0	20 (74.1)
Fatigue	13 (48.1)	5 (18.5)	1 (3.7)	0	19 (70.4)
Hypertension	0	13 (48.1)	5 (18.5)	0	18 (66.7)
AST increased	12 (44.4)	2 (7.4)	3 (11.1)	0	17 (63.0)
Headache	17 (63.0)	0	0	0	17 (63.0)
Proteinuria	5 (18.5)	10 (37.0)	2 (7.4)	0	17 (63.0)
ALT increased	10 (37.0)	3 (11.1)	2 (7.4)	0	15 (55.5)
Diarrhea	9 (33.3)	4 (14.8)	2 (7.4)	0	15 (55.5)
Blood LDH increased	10 (37.0)	2 (7.4)	2 (7.4)	0	14 (51.9)
Blood albumin decreased	8 (29.6)	5 (18.5)	0	0	13 (48.1)
Blood alkaline phosphatase increased	11 (40.7)	1 (3.7)	1 (3.7)	0	13 (48.1)
Anorexia	7 (25.9)	4 (14.8)	1 (3.7)	0	12 (44.4)
Nausea	10 (37.0)	1 (3.7)	1 (3.7)	0	12 (44.4)
GGT increased	3 (11.1)	6 (22.2)	2 (7.4)	0	11 (40.7)
Platelet count decreased	5 (18.5)	3 (11.1)	3 (11.1)	0	11 (40.7)
Blood fibrinogen increased	10 (37.0)	0	0	0	10 (37.0)
Odema peripheral	9 (33.3)	1 (3.7)	0	0	10 (37.0)
Nasopharyngitis	9 (33.3)	0	0	0	9 (33.3)
Protein total decreased	9 (33.3)	0	0	0	9 (33.3)
Vomiting	5 (18.5)	2 (7.4)	1 (3.7)	0	8 (29.6)
Blood creatinine decreased	5 (18.5)	2 (7.4)	0	0	7 (25.9)
Blood TSH increased	6 (22.2)	1 (3.7)	0	0	7 (25.9)
Blood urea increased	7 (25.9)	0	0	0	7 (25.9)
Constipation	7 (25.9)	0	0	0	7 (25.9)
Dyspnea	5 (18.5)	0	2 (7.4)		7 (25.9)
WBC count increased	3 (11.1)	4 (14.8)	0	0	7 (25.9)
Anemia	3 (11.1)	1 (3.7)	2 (7.4)	0	6 (22.2)
Dizziness	6 (22.2)	0	0	0	6 (22.2)
Hyperlipidemia	1 (3.7)	4 (14.8)	1 (3.7)	0	6 (22.2)

Abbreviations: GGT, γ-glutamyltransferase; TSH, thyroid stimulating hormone; WBC, white blood cells.

(66.7%), AST increased (63.0%), headache (63.0%), proteinuria (63.0%), ALT increased (55.5%), diarrhea (55.5%), and lactate dehydrogenase (LDH) increased (51.9%; Table 2).

Five patients experienced 6 serious AEs (SAEs) considered to be related or possibly related to study medication, which included hypertension (0.5 and 6 mg bid), hemorrhage (6 mg bid), pneumonia and worsening dyspnea (9 mg bid) and platelet count decrease (9 mg bid).

In total, 27 dose reductions were recorded, 3 each at 0.5, 1, 2, 4, 9, and 13 mg bid doses and 4 at the 6 mg dose. One patient who received 6 mg bid discontinued the study due to postrenal failure AE. One patient died due to worsening underlying disease during the study.

Pharmacokinetics

All patients had measurable plasma E7080 concentrations (>0.08 ng/mL) up to 168 hours after administration of either a single oral E7080 dose, or after 14 days of twice daily E7080 administration. Although the concentration was below the limit of quantification in 5 samples at 168 hours after single last dose, they did not affect the overall analysis. Maximal plasma concentration (C_{max}), the time to peak plasma concentration (t_{max}) and elimination half-life ($t_{1/2}$) for E7080 after a single dose and during steady state (ss) were similar (Table 3). C_{ssmax} and area under the plasma concentration–time curve (AUC) from time zero to the last measurable concentration ($AUC_{0-\tau}$) were dose proportional (Fig. 1).

The serum protein binding rates ranged from 96.6% to 98.2%. The previously reported IC_{50} of E7080 for VEGFR-2 phosphorylation in EC was 0.83 nmol/L (11), which based on 96.6% to 98.2% of E7080 being protein bound is approximately equivalent to a plasma concentration of 17 ng/mL. The IC_{50} of E7080 in plasma was almost equivalent to a maximum plasma concentration (C_{max}) at 0.5 mg bid and to a minimum plasma concentration (C_{min}) at 2 mg bid in multiple dosing (Table 2). After

Table 3. Pharmacokinetic parameters for E7080 following single administration on day 1 of a 21-day cycle (cycle 0) and twice daily on days 1 to 14[a] of a 21-day cycle (cycle 1)

Parameter[b]	E7080 dose levels, mg bid										
	0.5	1	2	4	6	9	13	16	20[c]		
Cycle 0 (single dose)[d]											
n	3	3	3	3	4	3	3	3		2	
C_{max}, ng/mL	2.5 (0.2)	5.3 (2.5)	18.4 (3.5)	61.3 (25.6)	99.3 (20.6)	201.4 (49.4)	302.7 (72.5)	471.5 (151.7)	329.2		674.2
t_{max}, h	5 (3–5)	3 (3–5)	3 (1–3)	1 (1–3)	3 (1–3)	1 (1–3)	1 (1–3)	1 (1–1)	3		3
AUC_{0-24}, ng h/mL	41 (2.0)	75 (30)	218 (33)	511 (111)	876 (165)	1,329 (379)	2,319 (339)	3,047 (597)	2,270		4,751
$AUC_{0-\infty}$, ng h/mL	115 (27)	164 (76)	429 (89)	759 (89)	1,202 (265)	1,658 (460)	2,744 (418)	3,419 (515)	2,849		5,405
$t_{½}$, h	46.5 (5.9)	30.3 (8.9)	36.4 (4.0)	32.0 (5.9)	31.6 (5.0)	28.6 (4.0)	25.0 (8.2)	19.1 (13.0)	38.1		31.6
Cycle 1 (multiple dosing)[e]											
n	3	3	3	3	3	3	3	3		1	
C_{ssmax}, ng/mL	16.7 (5.2)	23.7 (9.4)	68.6 (23.3)	154.0 (33.8)	178.2 (38.0)	384.4 (168.5)	556.8 (108.7)	713.3 (276.8)	393.5		–
C_{ssmin}, ng/mL	7.2 (2.6)	9.5 (4.6)	20.3 (3.8)	39.6 (7.7)	57.1 (21.4)	74.4 (32.6)	138.3 (40.1)	149.4 (52.5)	85.0		–
t_{maxss}, h	1 (1–3)	3 (3–3)	1 (1–3)	3 (1–3)	3 (1–6)	1 (1–1)	3 (1–3)	3 (1–3)	3		–
$AUC_{0-\tau}$, ng·h/mL	128 (36)	198 (86)	483 (117)	1,022 (246)	1,186 (141)	2,169 (803)	3,824 (622)	4,228 (1,485)	2,519		–
$t_{½ss}$, h	37.1 (1.0)	32.7 (3.4)	36.3 (6.4)	36.3 (1.7)	32.6 (2.5)	32.8 (2.7)	32.6 (6.8)	25.6 (7.1)	38.5		–

[a]E7080 administered only in the morning of day 14, cycle 1.

[b]Data are shown as mean (SD), except for t_{max} and t_{maxss} which are median (range).

[c]For E7080 20 mg bid, individual values are displayed for each patient.

[d]The pharmacokinetic profile was evaluated in cycle 0 after single dosing in 26 patients.

[e]The pharmacokinetic profile was evaluated in cycle 1 after multiple dosing in 25 patients.

Published OnlineFirst March 3, 2011; DOI:10.1158/1078-0432.CCR-10-2638

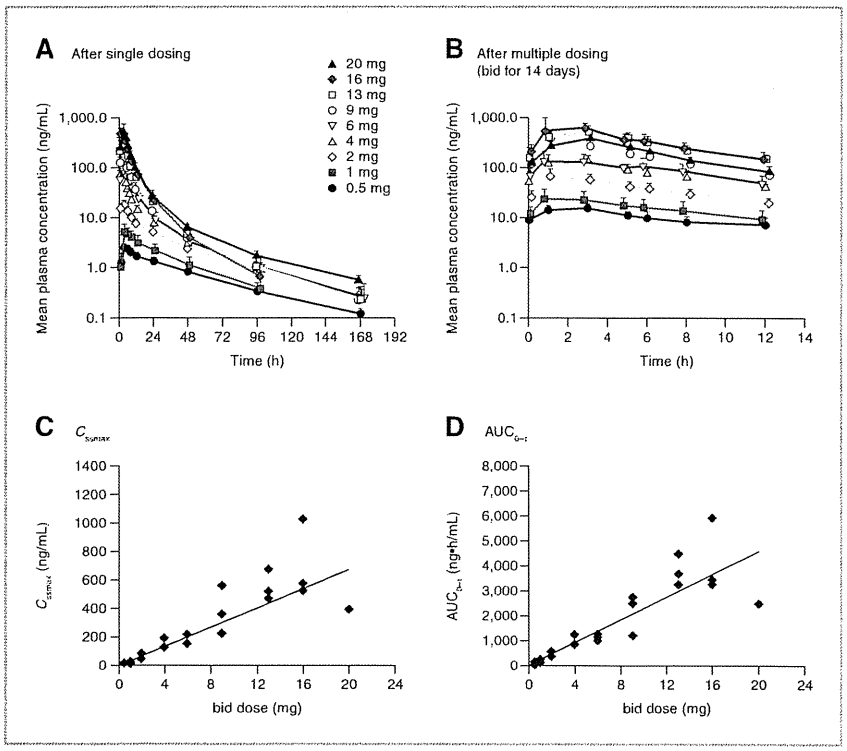

Figure 1. Pharmacokinetic profile of E7080. Plasma concentration-time profiles (A) after single dosing and (B) after multiple dosing. Data shown as mean + SD. Dose-dependent increase of (C) C_{trnax} and (D) $AUC_{0-\tau}$ at ss after multiple dosing.

repeated E7080 administration, urinary excretion of the parent compound ($fe_{0-\tau}$) ranged from 0.5% to 2.0%, and renal clearance was 17.4 to 84.6 mL/h, with no uniform trends observed across the dose range studied.

Antitumor activity

In 9 dose cohorts ranging from 0.5 to 20 mg bid, 27 patients received E7080 treatment for a median of 4.0 cycles (range 1–12). The median treatment duration was 86.0 days (range 1–270). Treatment duration was independent of E7080 dose level. Of 26 patients in the efficacy population, 25 were evaluable for response by RECIST. A partial response was documented in 1 patient with colon cancer at cycle 4 of E7080 2 mg bid which continued until cycle 10, when progressive disease was reported. Stable disease was recorded as best overall response in 21 patients, 84% of the evaluable patients.

Pharmacodynamics

Change in CEP and CEC number and correlation with E7080 therapeutic effect. The total number of CEPs decreased after 14 days' treatment with E7080 ($P < 0.001$). However, only the number of c-kit(+) CEPs decreased significantly ($P < 0.001$), and c-kit(−) CEP number was not affected (Fig. 2A). In contrast, while no change was seen in the total number of CECs, c-kit(+) CECs decreased significantly ($P < 0.01$) and c-kit(−) CECs increased significantly ($P < 0.001$; Fig. 2B). The c-kit(+) ratio in both CEP and CEC populations decreased upon E7080 treatment (Fig. 2C, D), although this was independent of E7080 dose (Fig. 2E, F). The reduction in c-kit(+) ratio in CECs associated with E7080 treatment correlated with treatment duration (Spearman's rank correlation coefficient $\rho = -0.468$; $P = 0.018$), while no correlation of c-kit(+) ratio in CEPs with treatment duration was observed (Fig. 2G, H).

Correlation of baseline biomarker levels with E7080 therapeutic effect

Significant inverse correlations were observed with E7080 treatment duration and baseline levels of c-kit(+) CEP and c-kit(+) ratio in CEP, but not CEC (Supplementary Table SA1). Similarly, analysis of baseline levels of angiogenic proteins and cytokines, including key CEP and CEC regulatory factors, revealed a significant inverse correlation with E7080 treatment duration and predose levels of plasma SDF1α (Supplementary Table SA2). These data suggest that patients with higher baseline levels of these biomarkers showed shorter treatment duration.

Discussion

In this Phase I dose escalation study, PK, PD, and preliminary efficacy of E7080 was investigated in patients

Published OnlineFirst March 3, 2011; DOI:10.1158/1078-0432.CCR-10-2638

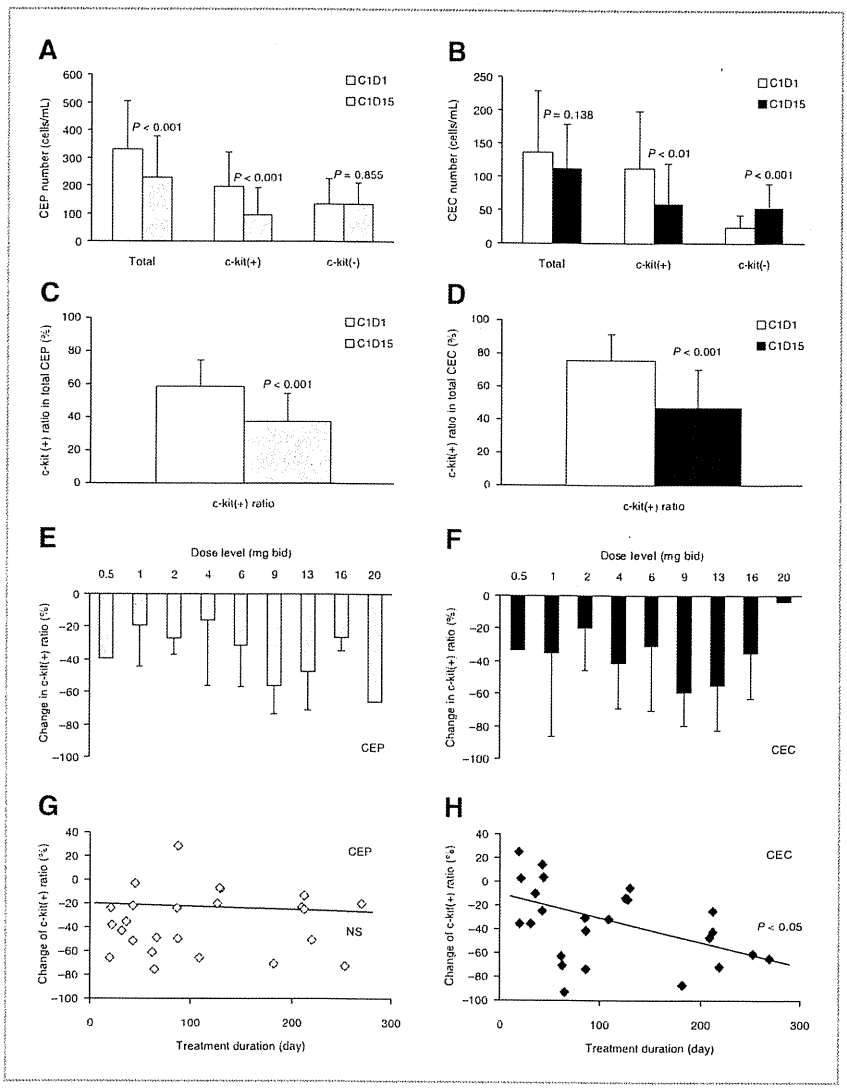

Figure 2. Decrease of CEP and CEC number associated with E7080 and correlation with treatment duration. A, 14-day E7080 treatment decreased total CEP, c-kit CEP, but not c-kit(−) CEP. B, E7080 treatment did not affect total CEC number, but decreased c-kit(+) CECs, and increased c-kit(−) CECs. C and D, E7080 decreased c-kit(+) ratio in CEP and CEC populations, respectively. Change in CEC and CEP number from cycle 1 day 1 (C1D1) to day 15 (C1D15) were statistically analyzed for each patient by Wilcoxon signed rank test. E and F, the decrease of c-kit(+) ratio was independent of E7080 dose level in CEP and CEC populations. G and H, the decrease in c-kit(+) ratio associated with E7080 correlated with treatment duration for CECs but not for CEPs. NS, not significant.

with advanced solid tumors. E7080 demonstrated a manageable toxicity profile at doses of 0.5 to 13 mg bid. Only 3 DLTs were reported, all with E7080 doses of 16 mg or more bid. Based on the occurrence of 1 DLT or more in the E7080 16 and 20 mg bid groups, 13 mg bid was considered to be the MTD when E7080 was administered in a 2-week-on/1-week-off cycle. The PK parameters of E7080, after repeated doses, were dose proportional within the dose range of 0.5 to 20 mg bid. The elimination half-life during ss was approximately 30 hours.

The previously reported IC_{50} of E7080 for VEGFR-2 phosphorylation in EC was 0.83 nmol/L (11), which is approximately equivalent to a plasma concentration of 17 ng/mL on the basis of 96.6% to 98.2% of E7080 being protein bound. The C_{min} reached the IC_{50} and the C_{max} was 4-fold higher than the IC_{50} at 2 mg bid. These data suggest that E7080 may suppress VEGFR-2 activity at doses of 2 mg or more bid during multiple dosing.

As reported in another clinical study of E7080 (23), hypertension and proteinuria were induced frequently (Table 2). These effects have been documented upon administration of several inhibitors of the VEGF signaling pathway, such as bevacuzimab and cediranib (24, 25), due to a possible perturbation of endothelial cell function (23). In this present study, hypertension was well managed by antihypertensive agents and proteinuria was managed by dose reductions or delays, and did not cause dose interruptions at the MTD or lower doses.

Published OnlineFirst March 3, 2011; DOI:10.1158/1078-0432.CCR-10-2638

The subpopulations of CEC and CEP may be predictive of disease or clinical responsiveness to anti-VEGF agents to a greater extent (26). E7080 has previously been shown to decrease the number of total CEC in tumor-bearing mice (11). In the study presented here, E7080 reduced the subpopulations of CEP and CEC that express c-kit, but did not reduce the number cells negative for c-kit expression from either subpopulation. C-kit and its ligand SCF are expressed on activated EC layers and play a key role in the survival and differentiation of cultured EC and in CEP recruitment during tumor angiogenesis (27, 28). E7080 may suppress the production of c-kit(+) CEP in bone marrow through inhibition of c-kit kinase, which may contribute to the antitumorigenic effects observed in this study (11).

Levels of biomarkers at baseline may be useful predictors of response and assist in selecting the most appropriate therapy for individual patients. Higher baseline CEC was correlated with delayed disease progression in patients with non–small cell lung and breast cancer (29, 30). We did not find a correlation between baseline CEC numbers and therapeutic effect, however significant correlations between baseline levels of SDF1, c-kit(+) CEP number and c-kit(+) ratio in CEC were shown with E7080 treatment duration. SDF1α and its receptor CXCR4 enhance CEP accumulation at angiogenic sites and are important in antiangiogenic therapy resistance (31, 32). Therefore, a high baseline level of SDF1α and c-kit(+) CEP may be a possible biomarker for predicting tumor resistance to E7080 treatment.

Dosing schedules of E7080 were evaluated in 2 other Phase I studies and a recommendation of 25 mg once daily or 10 mg bid without treatment-off period was made (33, 34). These studies also reported DLTs of grade 2 or less proteinuria and hypertension, as well as low incidences of grade 3/4 hemorrhage and thrombosis, tachycardia and fatigue (33, 34). Recent analysis has indicated that no difference between qd and bid regimen is observed with respect to exposure safety and efficacy (35). However, E7080 at 25 mg qd was recommended for future studies as this dose allows the targeting of higher exposures compared to 10 mg bid (35). A number of Phase II studies are currently recruiting or underway and the most common dosing regimen employed is 24 mg qd, although several studies are being initiated with dose-finding Phase I trials (NCT00784303, NCT01111461, NCT01136967, NCT01137604, NCT01133756, NCT00946153, NCT01133977, NCT01136733; www.clinicaltrials.gov).

In conclusion, this Phase I study has shown that E7080 was generally well tolerated and determined the MTD as 13 mg bid when administered in a 2-week-on/1-week-off cycle. Biomarker analyses suggest an antiangiogenic activity correlated with therapeutic effect in patients with a wide range of solid tumors. Studies are warranted to continue the evaluation of E7080 clinical efficacy and safety.

Disclosure of Potential Conflicts of Interest

No potential conflicts of interest were disclosed.

Acknowledgments

The authors thank Yuki Nishioka and Kenichi Saito (Eisai Co., Ltd) for the PK and PD parameter analyses. They thank Fiona Boswell of Complete Medical Communications, who provided medical writing support funded by Eisai, Inc. They also thank the commitment of participating patients, their families, and the study investigators for their invaluable contribution to this research.

Grant Support

This study was funded by Eisai Co. Ltd.

The costs of publication of this article were defrayed in part by the payment of page charges. This article must therefore be hereby marked *advertisement* in accordance with 18 U.S.C. Section 1734 solely to indicate this fact.

Received October 1, 2010; revised January 14, 2011; accepted February 7, 2011; published OnlineFirst March 3, 2011.

References

1. Ellis LM, Hicklin DJ. VEGF-targeted therapy: mechanisms of anti-tumour activity. Nat Rev Cancer 2008;8:579–91.
2. Hoffmann J, Feng Y, vom Hagen F, Hillenbrand A, Lin J, Erber R, et al. Endothelial survival factors and spatial completion, but not pericyte coverage of retinal capillaries determine vessel plasticity. FASEB J 2005;19:2035–6.
3. Koyama N, Hart CE, Clowes AW. Different functions of the platelet-derived growth factor-alpha and -beta receptors for the migration and proliferation of cultured baboon smooth muscle cells. Circ Res 1994;75:682–91.
4. Knights V, Cook SJ. De-regulated FGF receptors as therapeutic targets in cancer. Pharmacol Ther 2010;125:105–17.
5. Watanabe S, Morisaki N, Tezuka M, Fukuda K, Ueda S, Koyama N, et al. Cultured retinal pericytes stimulate in vitro angiogenesis of endothelial cells through secretion of a fibroblast growth factor-like molecule. Atherosclerosis 1997;130:101–7.
6. Ellis LM, Hicklin DJ. Resistance to targeted therapies: refining anticancer therapy in the era of molecular oncology. Clin Cancer Res 2009;15:7471–8.
7. Jubb AM, Oates AJ, Holden S, Koeppen H. Predicting benefit from anti-angiogenic agents in malignancy. Nat Rev Cancer 2006;6:626–35.
8. Wong CI, Koh TS, Soo R, Hartono S, Thng CH, McKeegan E, et al. Phase I and biomarker study of ABT-869, a multiple receptor tyrosine kinase inhibitor, in patients with refractory solid malignancies. J Clin Oncol 2009;27:4718–26.
9. Yamamoto N, Tamura T, Yamamoto N, Yamada K, Yamada Y, Nokihara H, et al. Phase I, dose escalation and pharmacokinetic study of cediranib (RECENTIN), a highly potent and selective VEGFR signalling inhibitor, in Japanese patients with advanced solid tumors. Cancer Chemother Pharmacol 2009;64:1165–72.
10. Fujisaka Y, Yamada Y, Yamamoto N, Shimizu T, Fujiwara Y, Yamada K, et al. Phase 1 study of the investigational, oral angiogenesis inhibitor motesanib in Japanese patients with advanced solid tumors. Cancer Chemother Pharmacol 2010 Jan 28. [Epub ahead of print].
11. Matsui J, Yamamoto Y, Funahashi Y, Tsuruoka A, Watanabe T, Wakabayashi T, et al. E7080, a novel inhibitor that targets multiple kinases, has potent antitumor activities against stem cell factor

Published OnlineFirst March 3, 2011; DOI:10.1158/1078-0432.CCR-10-2638

producing human small cell lung cancer H146, based on angiogenesis inhibition. Int J Cancer 2008;122:664–71.
12. Matsui J, Funahashi Y, Uenaka T, Watanabe T, Tsuruoka A, Asada M. Multi-kinase inhibitor E7080 suppresses lymph node and lung metastases of human mammary breast tumor MDA-MB-231 via inhibition of vascular endothelial growth factor-receptor (VEGF-R) 2 and VEGF-R3 kinase. Clin Cancer Res 2008;14:5459–65.
13. Ikuta K, Yano S, Trung VT, Hanibuchi M, Goto H, Li Q, et al. E7080, a multi-tyrosine kinase inhibitor, suppresses the progression of malignant pleural mesothelioma with different proangiogenic cytokine production profiles. Clin Cancer Res 2009;15:7229–39.
14. Chang YS, Adnane J, Trail PA, Levy J, Henderson A, Xue D, et al. Sorafenib (BAY 43–9006) inhibits tumor growth and vascularization and induces tumor apoptosis and hypoxia in RCC xenograft models. Cancer Chemother Pharmacol 2007;59:561–74.
15. Mendel DB, Laird AD, Xin X, Louie SG, Christensen JG. Li G, et al. *In vivo* antitumor activity of SU11248, a novel tyrosine kinase inhibitor targeting vascular endothelial growth factor and platelet-derived growth factor receptors: determination of a pharmacokinetic/pharmacodynamic relationship. Clin Cancer Res 2003;9:327–37.
16. Cockcroft DW, Gault MH. Prediction of creatinine clearance from serum creatinine. Nephron 1976;16:31–41.
17. Trotti A, Colevas AD, Setser A, Rusch V, Jaques D, Budach V, et al. CTCAE v3.0: development of a comprehensive grading system for the adverse effects of cancer treatment. Semin Radiat Oncol 2003;13: 176–81.
18. Tsuchida Y, Therasse P. Response evaluation criteria in solid tumors (RECIST): new guidelines. Med Pediatr Oncol 2001;37:1–3.
19. Bertolini F, Shaked Y, Mancuso P, Kerbel RS. The multifaceted circulating endothelial cell in cancer: towards marker and target identification. Nat Rev Cancer 2005;6:835–45.
20. Duda DG, Cohen KS, di Tomaso E, Au P, Klein RJ, Scadden DT, et al. Differential CD146 expression on circulating versus tissue endothelial cells in rectal cancer patients: implications for circulating endothelial and progenitor cells as biomarkers for antiangiogenic therapy. J Clin Oncol 2006;24:1449–53.
21. Kimura H, Kasahara K, Sekijima M, Tamura T, Nishio K. Plasma MIP-1beta levels and skin toxicity in Japanese non-small cell lung cancer patinets treated with the EGFR-targeted tyrosine kinase inhibitor, gefitinib. Lung Cancer 2005;50:393–9.
22. Drevs J, Siegert P, Medinger M, Mross K, Strecker R, Zirrgiebel U, et al. Phase I clinical study of AZD2171, an oral vascular endothelial growth factor signaling inhibitor, in patients with advanced solid tumors. J Clin Oncol 2007;25:3045–54.
23. Keizer RJ, Gupta A, Mac Gillavry MR, Jansen M, Wanders J, Beijnen JH, et al. A model of hypertension and proteinuria in cancer patients treated with the anti-angiogenic drug E7080. J Pharmacokinet Pharmacodyn 2010;37:347–63.
24. Robinson ES, Matulonis UA, Ivy P, Berlin ST, Tyburski K, Penson RT, et al. Rapid development of hypertension and proteinuria with cediranib, an oral vascular endothelial growth factor receptor inhibitor. Clin J Am Soc Nephrol 2010;5:477–83.
25. Zhu X, Wu S, Dahut WL, Parikh CR. Risks of proteinuria and hypertension with bevacizumab, an antibody against vascular endothelial growth factor: systematic review and meta-analysis. Am J Kidney Dis 2007;49:186–93.
26. Ronzoni M, Manzoni M, Mariucci S, Loupakis F, Brugnatelli S, Bencardino K, et al. Circulating endothelial cells and endothelial progenitors as predictive markers of clinical response to bevacizumab-based first-line treatment in advanced colorectal cancer patients. Ann Oncol 2010;21:2382–9.
27. Matsui J, Wakabayashi T, Asada M, Yoshimatsu K, Okada M. Stem cell factor/c-kit signaling promotes the survival, migration, and capillary tube formation of human umbilical vein endothelial cells. J Biol Chem 2004;279:18600–7.
28. Dentelli P, Rosso A, Balsamo A, Colmenares Benedetto S, Zeoli A, Pegoraro M, et al. C-KIT, by interacting with the membrane-bound ligand, recruits endothelial progenitor cells to inflamed endothelium. Blood 2007;109:4264–71.
29. Kawaishi M, Fujiwara Y, Fukui T, Kato T, Yamada K, Ohe Y, et al. Circulating endothelial cells in non-small cell lung cancer patients treated with carboplatin and paclitaxel. J Thorac Oncol 2009;4:208–13.
30. Calleri A, Bono A, Bagnardi V, Quarna J, Mancuso P, Rabascio C, et al. Predictive potential of angiogenic growth factors and circulating endothelial cells in breast cancer patients receiving metronomic chemotherapy plus bevacizumab. Clin Cancer Res 2009;15:7652–7.
31. Takahashi M. Role of the SDF-1/CXCR4 system in myocardial infarction. Circ J 2010;74:418–23.
32. Jain RK, Duda DG, Willett CG, Sahani DV, Zhu AX, Loeffler JS, et al. Biomarkers of response and resistance to antiangiogenic therapy. Nat Rev Clin Oncol 2009;6:327–38.
33. Glen H, Boss DR, Morrison R, et al. A phase I study of E7080 in patients (pts) with advanced malignancies. J Clin Oncol 2008;26:abstr 3526.
34. Hong DS, Koetz BS, Kurzrock R, et al. Phase I dose-escalation study of E7080, a selective tyrosine kinase inhibitor, administered orally to patients with solid tumors. J Clin Oncol 2010;28:abstr 2540.
35. Gupta A, Koetz B, Hanekom W. Population pharmacokinetics and exposure/ response relationship of the receptor tyrosine kinase inhibitor E7080 in phase I studies. Presented at the 22nd EORTC-NCI-AACR symposium on "Molecular targets and Cancer Therapeutics, 2010, abstr 453.

Cancer Science
The official journal of the Japanese Cancer Association JCA

Phase I study of intravenous ASA404 (vadimezan) administered in combination with paclitaxel and carboplatin in Japanese patients with non-small cell lung cancer

Toyoaki Hida,[1,7] Motohiro Tamiya,[2] Makoto Nishio,[3] Nobuyuki Yamamoto,[4] Tomonori Hirashima,[2] Takeshi Horai,[3] Hiromi Tanii,[5] Michael M. Shi,[6] Ken Kobayashi[5] and Yoshitsugu Horio[1]

[1]Aichi Cancer Center Hospital, Aichi; [2]Osaka Prefectural Medical Center for Respiratory and Allergic Diseases, Osaka; [3]Cancer Institute Hospital, Tokyo; [4]Shizuoka Cancer Center, Shizuoka; [5]Novartis Pharma K.K., Tokyo, Japan; [6]Novartis Pharmaceuticals Corporation, New Jersey, USA

(Received October 27, 2010/Revised December 14, 2010/Accepted December 15, 2010/Accepted manuscript online December 23, 2010/Article first published online February 8, 2011)

ASA404 (5,6-dimethylxanthenone-4-acetic acid, vadimezan), a flavone-8-acetic acid analogue, is a novel tumor-vascular disrupting agent. In this study, the safety and tolerability, pharmacokinetics and pharmacodynamics of ASA404 in combination with standard therapy of paclitaxel and carboplatin (P/C) were assessed. A total of 15 Japanese patients with stage IV advanced non-small cell lung cancer were enrolled and P/C plus ASA404 at three dose levels (600–1800 mg/m^2) was administered every 3 weeks. Dose limiting toxicities were observed in two patients during Cycle 1 of ASA404 treatment (Grade 3 febrile neutropenia at ASA404 1200 mg/m^2 and Grade 3 QT prolongation at ASA404 1800 mg/m^2) and the incidence of dose limiting toxicity was ≤1/3. The most frequently reported adverse events were injection site pain, peripheral sensory neuropathy, alopecia, neutropenia, nausea, anorexia and arthralgia, which were similar to those seen in previous Phase I/II studies. Pharmacokinetic analysis revealed the plasma area under the curve (AUC) of total ASA404 increased in a mostly dose-proportional manner within the dose range investigated. Administration of ASA404 raised plasma 5-hydroxyindole-3-acetic acid level dose-dependently by 116 and 204% after 1200 and 1800 mg/m^2 doses, respectively. Partial response was observed in four patients (27%), and seven patients (47%) exhibited stable disease. Overall, the safety and preliminary efficacy profiles were comparable to those seen in non-Japanese patients in previous Phase I and Phase II studies, and support the further evaluation of ASA404 (1800 mg/m^2) in Phase III studies in combination with P/C in Japanese patients with advanced non-small cell lung cancer. (*Cancer Sci* 2011; 102: 845–851)

Worldwide, over 1.3 million people are diagnosed each year with lung cancer, with over 1.1 million deaths.[1,2] Non-small cell lung cancer (NSCLC) accounts for 87% of all lung cancers, with most patients diagnosed at advanced stages for which the 5-year survival rate is poor (<5%).[3,4] Lung cancer is also a disease that predominantly affects the elderly, with most cases (85%) occurring in patients over 60 years of age.[5] In Japan alone, the number of newly diagnosed patients with NSCLC reached 85 000 by 2005, and 45 927 Japanese men and 17 307 women died from the disease in 2006.[6,7] Current standard treatments are usually platinum-based combination therapies, and platinum-taxane regimens predominate in Japan (>55%).[8] These treatment regimens extend survival but are rarely curative,[9,10] and there remains a need for more effective and better tolerated therapies.

Like all solid tumors, lung tumors depend upon a functional vascular supply to meet demand for oxygen and nutrients required for growth and development.[11] Furthermore, a high level of vascularity in peripheral lung tumor tissue has been shown to correlate with lung cancer progression.[12] Microvessel density in lung cancers is also a prognostic indicator of metastasis and poor survival.[13–15] The vasculature of solid tumors is typified by aberrant vessels, the unique characteristics of which present an opportunity for selective therapeutic intervention.[16,17] ASA404 (vadimezan), a flavone-8-acetic acid analogue, is a tumor-vascular disrupting agent (tumor-VDA) that selectively targets the immature and rapidly proliferating endothelial cells of established tumor vasculature.[18] ASA404 induces rapid tumor endothelial cell apoptosis and a cascade of events that induces a sustained effect on tumor blood flow, causing hypoxia, vascular failure, and inflammatory responses.[18–22] These effects lead to extensive tumor necrosis,[23] although a viable rim of surviving cells remains at the tumor periphery when the agent is used alone.[24] The activity of ASA404, which causes necrosis at the tumor core, may thus be maximized by combining it with chemotherapeutic agents, which often have greatest effect at the tumor periphery. Preclinical studies on ASA404 combined with various chemotherapeutic agents have demonstrated enhanced anti-tumor activity compared with chemotherapy alone. This synergy is most notable with taxanes,[25–27] and studies in combination with paclitaxel in human NSCLC xenografts have produced tumor cures.[25,28]

Three Phase I clinical studies with ASA404 established a maximum tolerated dose of 3700 mg/m^2, with dose-limiting toxicities (DLTs) occurring at doses of 4900 mg/m^2.[29–31] Side effects were relatively mild, and only transient, with moderate cardiac changes occurring at higher doses.[29,30] Visual disturbances were also reported in these studies but only at the highest doses (≥2400 mg/m^2).[29–31] A dose of 1200 mg/m^2 was selected for a randomized Phase II study to determine the feasibility of combining ASA404 with paclitaxel and carboplatin (P/C). The study (n = 37) examined the potential for pharmacokinetic (PK) interactions between components of this regimen and evaluated its safety and efficacy in patients with previously untreated advanced NSCLC.[32] The ASA404 combination improved a range of efficacy endpoints compared with P/C alone—most notably overall survival (14.0 months in the P/C + ASA404 [1200 mg/m^2] group vs 8.8 months for P/C alone). The risk of death was reduced by 27% (hazard ratio [HR] = 0.73, 95% confidence interval [CI]: 0.39, 1.38) with a response rate of 31 vs 22% for P/C alone.[32] A single-arm extension of this study (n = 29) subsequently elevated the ASA404 dose to 1800 mg/m^2, which was well tolerated, and a

[7]To whom correspondence should be addressed. E-mail: 107974@aichi-cc.jp

doi: 10.1111/j.1349-7006.2010.01839.x

median survival of 14.9 months was demonstrated.[33] Safety and efficacy endpoints were also similar in both squamous and non-squamous patients.[34] Phase II evaluations have shown that ASA404 is a promising addition to standard NSCLC chemotherapy but this must be confirmed in a larger prospective study. The Phase III study of ASA404 as a first-line treatment for NSCLC in combination with P/C (ATTRACT-1) was halted following interim data analysis showing futility. However, no safety concerns were identified.[35]

The primary objective of this open-label, non-randomized, sequential dose escalation Phase I study was to assess the safety profile and tolerability of ASA404 when administered in combination with fixed doses of P/C in Japanese patients with previously untreated, stage IIIb/IV advanced NSCLC. Secondary objectives were to characterize the PK profile in Japanese patients, to assess pharmacodynamic (PD) effects and evaluate preliminary anti-tumor activity.

Materials and Methods

Patient population. Japanese patients ≥20 years of age with newly diagnosed, histologically or cytologically confirmed, stage IIIb/IV NSCLC were eligible for inclusion. Other requirements were that patients had no prior treatment for stage IIIb/IV disease (prior neoadjuvant or adjuvant chemotherapy within 6 months was allowed), World Health Organization (WHO) performance status (PS) of 0–1 and life expectancy ≥12 weeks. Eligible patients could have either squamous or non-squamous histology.

Specific criteria for exclusion were: symptomatic central nervous system (CNS) metastases requiring treatment; second primary cancer with the exception of non-melanoma skin cancer or cervical cancer *in situ*; radiotherapy (unless palliative) within 4 weeks; major surgery within 4 weeks; prior exposure to tumor-VDAs or other vascular targeting agents; pleural effusion requiring drainage; hemoptysis associated with NSCLC; long QT syndrome; myocardial infarction within 12 months; poorly controlled angina pectoris; ventricular tachycardia; history of ventricular fibrillation or torsades de pointes and use of medication known to prolong the QT interval.

Dosing and administration. The dose of ASA404 was selected based on the current data from clinical studies held in western countries. ASA404 was administered at doses of 600, 1200 and 1800 mg/m^2 as a 20 min intravenous (IV) infusion following infusion of paclitaxel (200 mg/m^2 IV over 3 h) and carboplatin (IV over 30 mins at a plasma AUC of 6 mg/ml × min) on day 1 of every cycle. Each treatment cycle span was 21 days and study treatment was administered for six cycles, although responding patients could proceed beyond six cycles. The initial dose of ASA404 was 600 mg/m^2, followed by dose escalation to 1200 mg/m^2, and then to 1800 mg/m^2. Evaluation at each dose level was performed based on data from at least three patients during cycle 1. If a DLT was confirmed during cycle 1 in one of the first three patients, the dose cohort was expanded by three additional patients for evaluation. Intrapatient dose escalation was not permitted for any patient. If the probability of DLT incidence was ≤1/3, escalation to the next dose level was performed. The recommended dose for the next phase was set as the highest achievable dose with a DLT incidence ≤1/3.

Safety assessments. The safety population comprised all patients who had received at least one dose of ASA404 and had at least one post-baseline safety assessment after drug administration. The dose-determining population included all patients from the safety population who either completed minimum safety evaluation requirements or discontinued due to DLT in cycle 1. Toxicity was evaluated according to the Common Terminology Criteria for Adverse Events, version 3.0 (Japanese version). A DLT was defined as a study drug-related adverse event (AE) including cardiac toxicity, QT prolongation, Grade 4 neutropenia (for >7 days), Grade 4 thrombocytopenia and persistent CNS toxicity, including ophthalmic toxicity, or abnormal laboratory value, occurring during cycle 1. Resumption of drug administration followed if dose modification criteria were met. No study drug dose reduction was permitted.

All patients were followed for AEs and serious AEs (SAEs) for 4 weeks following the last dose of ASA404. Patients whose treatment was permanently discontinued due to an AE or abnormal laboratory value were followed at least once a week for 4 weeks. SAEs or events that had a suspect relationship to study drug, were followed at 4 week intervals, until resolution or stabilization of the event, whichever came first. Visual disturbances were assessed in all patients at baseline and end of treatment.

Pharmacokinetic and pharmacodynamic analyses. To characterize the PK profile of ASA404, plasma concentrations of total (sum of plasma protein bound and unbound) ASA404 were measured during cycle 1 (immediately prior to infusion, <1 min before the end of infusion, and at 0.5, 1, 2, 4, 6, 24 and 48 h time points after infusion) and cycles 2–6 (immediately prior to infusion, <1 min before the end, and 1 and 4 h after infusion). Free (protein unbound) plasma ASA404 concentrations were also measured in cycle 1 only. Previous studies have shown that co-administration of ASA404 does not fundamentally alter the PK parameters of either paclitaxel or carboplatin.[32]

Urinary excretion was determined at cycle 1 day 1 (prior to infusion, start of infusion to 6 h post-infusion, and 6–24 h post-infusion) and cycle 1 day 2 (24–48 h post-infusion). Concentrations of ASA404 in plasma and urine were determined by liquid chromatography/tandem mass spectroscopy. Pharmacokinetic parameters were calculated by a non-compartmental method using WinNonlin Professional Edition (Pharsight, St. Louise, MO, USA) by lead PK analyst.

Plasma was also collected to evaluate the PD of ASA404 and determine whether markers predictive of activity could be defined. The ASA404-induced vascular damage biomarker, 5-hydroxyindole-3-acetic acid (5-HIAA) was determined, together with the angiogenesis markers, vascular endothelial growth factor (VEGF), placental growth factor, soluble VEGF receptors-1 and -2 (sVEGFR-1 and -2) and basic fibroblast growth factor. These samples were taken on cycle 1 day 1 at pre-study treatment, post-P/C dosing but pre-study drug infusion, 4 h post-study drug infusion and 24 h post-study drug infusion; and on cycle 2 day 1, cycle 4 day 1 and cycle 6 day 1 at pre-study treatment, post-carboplatin but pre-study drug infusion, and 1 h post-study drug infusion. In addition, a single blood collection was taken at the end of treatment visit.

Efficacy assessments. Efficacy was determined using the full analysis population of all patients who had received at least one dose of ASA404 according to the intention to treat principle. Tumor response was assessed in patients with measurable disease at baseline according to response evaluation criteria in solid tumors (RECIST) criteria, performed within 28 days before start of treatment. Tumor assessment was every 6 weeks and at the end of study. Best overall response in each patient was evaluated as complete response, partial response, progressive disease or stable disease. The objective response rate in this study was evaluated as the number of patients with complete response or partial response.

Results

Accrual and patient characteristics. A total of 15 patients with NSCLC were recruited and baseline characteristics are shown in Table 1. The majority of patients (60%) had adenocarcinoma, 13% had squamous cell carcinoma, and all patients had stage IV

doi: 10.1111/j.1349-7006.2010.01839.x

Table 1. Patient baseline characteristics

	P/C + ASA404 600 mg/m^2 n = 3	P/C + ASA404 1200 mg/m^2 n = 6	P/C + ASA404 1800 mg/m^2 n = 6	All subjects n = 15
Sex n (%)				
Female	1 (33)	5 (83)	2 (33)	8 (53)
Male	2 (67)	1 (17)	4 (67)	7 (47)
Age (years)				
Mean ± SD	57.3 ± 12.66	62.8 ± 6.27	60.2 ± 2.56	60.7 ± 6.62
WHO PS n (%)				
0	1 (33)	0 (0)	3 (50)	4 (27)
1	2 (67)	6 (100)	3 (50)	11 (73)
Histology/cytology n (%)				
Adenocarcinoma	1 (33)	4 (67)	4 (67)	9 (60)
Squamous cell carcinoma	0 (0)	1 (17)	1 (17)	2 (13)
Other	2 (67)	1 (17)	1 (17)	4 (27)
Stage n (%)				
Stage III	0 (0)	0 (0)	0 (0)	0 (0)
Stage IV	3 (100)	6 (100)	6 (100)	15 (100)
Prior antineoplastic therapy	1 (33)	2 (33)	0 (0)	3 (20)

P/C, paclitaxel and carboplatin; SD, standard deviation; WHO PS, World Health Organization Performance Status.

disease. WHO performance status (PS) was predominantly PS = 1 (73%). Approximately 70% of patients received a third course of ASA404 treatment.

Safety. Two patients exhibited DLT during cycle 1 of ASA404 treatment: one of six patients at a dose of 1200 mg/m^2 had Grade 3 febrile neutropenia and one of six patients at a dose of 1800 mg/m^2 had Grade 3 QT prolongation (the event resolved by day 6 of cycle 1; patient was discontinued).

The AEs observed were as expected for this population and for this class of drug,[29–33] and were experienced by all patients. The most frequently reported AEs by system organ class (SOC) were blood and lymphatic disorders, general disorders and administration site conditions, and nervous system disorders (n = 15, all 100% incidence). Blood and lymphatic disorders (n = 15, 100%) consisted of neutropenia including one neutrophil count decreased (n = 13, 87%), anemia (n = 9, 60%), thrombocytopenia (n = 4, 27%), and lymphopenia (n = 3, 20%). The most frequently reported Grade 3 or 4 hematological abnormality as a laboratory parameter was reduction in absolute neutrophils. The most common AEs of any grade were injection site pain, peripheral sensory neuropathy and alopecia, each occurring in 14 (93%) patients across all doses (Table 2). These events were mostly Grade 1 or 2, and resolved without treatment or concomitant medications. Other frequently occurring AEs were neutropenia, including one neutrophil count decreased (n = 13), anorexia (n = 12), arthralgia (n = 12), and nausea (n = 12). Grade 3 febrile neutropenia was reported as DLT in one patient, but Grade 3 or 4 AEs occurred with low frequency (<15%) with the exception of neutropenia (87% over all doses, including reduced neutrophil count and febrile neutropenia) and are presented in Table 3.

Serious adverse events occurred in six patients, five of which occurred during the study, with none occurring at the lowest dose level of 600 mg/m^2, four at 1200 mg/m^2 and two at 1800 mg/m^2. All these SAEs occurred in one patient each, were not clustered in any particular primary system organ class and consisted of hemorrhagic enterocolitis, femoral neck fracture, pneumonia, pharyngitis and tumor hemorrhage. Seven patients discontinued the study due to AEs (three at the 1200 mg/m^2 dose and four at 1800 mg/m^2). No deaths were reported during the study, but one patient died more than 40 days after the last administration of ASA404 1800 mg/m^2 due to acute myocardial infarction.

Electrocardiogram (ECG)-evaluated QT prolongation occurred in three patients and T-wave inversion in one patient treated with ASA404. QT prolongation was reported in two patients who received P/C + ASA404 1800 mg/m^2, one of which was Grade 3 and judged as a DLT. However, both events were

Table 2. Frequently occurring (≥33% in all patients) adverse events of any grade, regardless of study drug relationship by preferred term

Adverse events	P/C + ASA404 600 mg/m^2 n = 3 (n, %)	P/C + ASA404 1200 mg/m^2 n = 6 (n, %)	P/C + ASA404 1800 mg/m^2 n = 6 (n, %)	All patients n = 15 (n, %)
Alopecia	2 (67)	6 (100)	6 (100)	14 (93)
Injection site pain	2 (67)	6 (100)	6 (100)	14 (93)
Peripheral sensory neuropathy	3 (100)	5 (83)	6 (100)	14 (93)
Neutropenia	3 (100)	6 (100)*	4 (67)	13 (87)
Anorexia	3 (100)	5 (83)	4 (67)	12 (80)
Arthralgia	3 (100)	5 (83)	4 (67)	12 (80)
Nausea	3 (100)	5 (83)	4 (67)	12 (80)
Fatigue	2 (67)	4 (67)	4 (67)	10 (67)
Anemia	2 (67)	4 (67)	3 (50)	9 (60)
Constipation	2 (67)	2 (33)	4 (67)	8 (53)
Myalgia	2 (67)	2 (33)	4 (67)	8 (53)
Diarrhea	2 (67)	2 (33)	1 (17)	5 (33)

*Including decreased neutrophil count. P/C, paclitaxel and carboplatin.

Table 3. Grade 3 or 4 adverse events, regardless of study drug relationship by preferred term

Adverse events	P/C + ASA404 600 mg/m^2 n = 3 (n, %)	P/C + ASA404 1200 mg/m^2 n = 6 (n, %)	P/C + ASA404 1800 mg/m^2 n = 6 (n, %)	All patients n = 15 (n, %)
Neutropenia	3 (100)	6 (100)*	4 (67)	13 (87)
Anemia	0 (0)	1 (17)	1 (17)	2 (13)
Anorexia	0 (0)	1 (17)	1 (17)	2 (13)
QT Prolongation	0 (0)	0 (0)	1 (17)	1 (7)
Enterocolitis hemorrhagic	0 (0)	1 (17)	0 (0)	1 (7)
Febrile neutropenia	0 (0)	1 (17)	0 (0)	1 (7)
Femoral neck fracture	0 (0)	1 (17)	0 (0)	1 (7)
Hyponatremia	0 (0)	1 (17)	0 (0)	1 (7)
Lymphopenia	0 (0)	1 (17)	0 (0)	1 (7)
Peripheral sensory neuropathy	0 (0)	0 (0)	1 (17)	1 (7)
Pneumonia	0 (0)	0 (0)	1 (17)	1 (7)

*Including decreased neutrophil count. P/C, paclitaxel and carboplatin.

asymptomatic and resolved within a short period (1 and 4 days, respectively) without treatment. There were no other cardiac events in this study.

No ophthalmic abnormalities were reported at ASA404 doses of 600 and 1200 mg/m^2; two incidences of dyschromatopsia occurred at the higher dose of 1800 mg/m^2. Visual acuity changes were not reported at any of the ASA404 dose levels used in this study.

Efficacy. The best overall response by investigator assessment was partial response, which was observed in four patients (27%), and seven patients (47%) exhibited stable disease. Response data are presented in Table 4.

Pharmacokinetics. Mean plasma concentration–time profiles of total and free ASA404 in cycle 1 are shown in Fig. 1, and a summary of PK parameters is given in Table 5. After reaching C_{max} at the end of infusion, plasma total ASA404 concentrations decreased biphasically over time at a dose of 600 mg/m^2, becoming more monophasic at higher doses, probably due to saturation of plasma protein binding. C_{max} increased dose proportionally from 600 to 1200 mg/m^2 but less than dose proportionally from 1200 to 1800 mg/m^2 (Fig. 2). The plasma AUC of total ASA404 was essentially dose-proportional over the range investigated (Fig. 2). Systemic clearance of total ASA404 decreased slightly with increasing dose from 3.88 L/h at 600 mg/m^2 to 2.87 and 2.78 L/h at doses of 1200 and 1800 mg/m^2, respectively (Table 5). Systemic clearance of free ASA404 was 20- to 50-fold higher than that of total ASA404 and the distribution volume of free ASA404 was 20- to 40-fold greater than that of total ASA404. Plasma protein binding of ASA404 was >93% and the free fraction in plasma decreased at lower total drug concentrations, indicating that protein binding is saturable. Mean urinary excretion of unchanged ASA404 was 6, 2 and 3% of the administered dose for 600, 1200 and 1800 mg/m^2, respectively, and mean renal clearance was 0.2, 0.07 and 0.08 L/h, respectively. Plasma concentrations of ASA404 did not alter at each cycle, indicating that there was no accumulation of ASA404 over repeated 3-weekly dosing, consistent with its observed short elimination half-life of 4.61–7.04 h.

Biomarker changes. *Effect of ASA404 on plasma 5-HIAA levels.* Plasma levels of the vascular damage PD biomarker 5-HIAA after infusion of P/C + ASA404 were evaluated on day 1 of cycle 1, 2, 4 and 6. Levels of 5-HIAA did not change after paclitaxel or carboplatin infusion, but were elevated 4 h after infusion of ASA404 at 1200 and 1800 mg/m^2, and were still

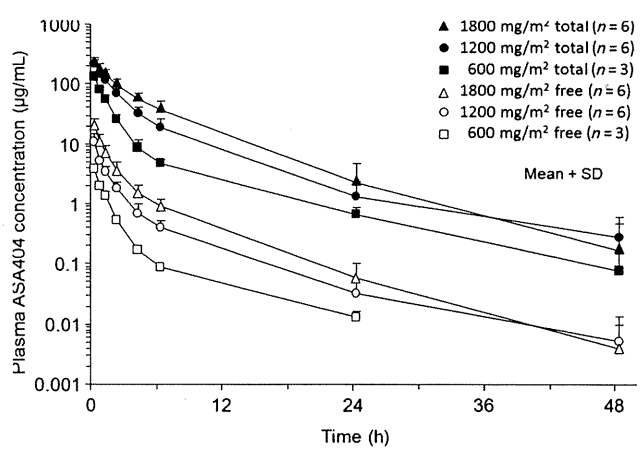

Fig. 1. Mean plasma concentration–time profiles of total and free ASA404 in cycle 1 of treatment; log-linear plot. SD, standard deviation.

Table 4. Best overall response observed by investigator assessment and RECIST criteria

Best overall response	P/C + ASA404 600 mg/m^2 n = 3 (n, %)	P/C + ASA404 1200 mg/m^2 n = 6 (n, %)	P/C + ASA404 1800 mg/m^2 n = 6 (n, %)	All patients n = 15 (n, %)
Complete response	0 (0)	0 (0)	0 (0)	0 (0)
Partial response	0 (0)	3 (50)	1 (17)	4 (27)
Stable disease	3 (100)	2 (33)	2 (33)	7 (47)
Progressive disease	0 (0)	1 (17)	3 (50)	4 (27)

P/C, paclitaxel and carboplatin; RECIST, response evaluation criteria in solid tumors.

doi: 10.1111/j.1349-7006.2010.01839.x

Table 5. Pharmacokinetic parameters

PK parameter		P/C + ASA404 600 mg/m^2 n = 3 (mean ± SD)	P/C + ASA404 1200 mg/m^2 n = 6 (mean ± SD)	P/C + ASA404 1800 mg/m^2 n = 6 (mean ± SD)
Total ASA404	T_{max} (h)	0.32 (0.28–0.33)†	0.31 (0.28–0.37)†	0.33 (0.30–0.35)†
	C_{max} (μg/mL)	137 ± 9.5	224 ± 33.8	247 ± 34.1
	$AUC_{0\text{-}inf}$ (μg*h/L)	260 ± 25.9	650 ± 97.2	1040 ± 137
	$t_{1/2}$ (h)	7.04 ± 1.06	5.86 ± 2.59	4.61 ± 1.07
	CL (L/h)	3.88 ± 0.77	2.87 ± 0.57	2.78 ± 0.55
	V_{ss} (L)	14.4 ± 3.12	11.7 ± 3.42	12.9 ± 4.93
Free ASA404	T_{max} (h)	0.32 (0.28–0.33)†	0.31 (0.28–0.37)†	0.33 (0.30–0.35)†
	C_{max} (μg/mL)	3.69 ± 0.74	11.0 ± 4.17	20.2 ± 6.03
	$AUC_{0\text{-}inf}$ (μg*h/L)	5.87 ± 0.97	18.7 ± 3.25	37.6 ± 9.46
	$t_{1/2}$ (h)	5.83 ± 0.13	5.68 ± 2.77	5.24 ± 1.92
	CL (L/h)	176 ± 53.7	101 ± 24.6	80.4 ± 28.2
	V_{ss} (L)	517 ± 171	318 ± 81.2	292 ± 227

†, median (range). AUC, area under the curve; CL, clearance; C_{max}, maximum plasma concentration; P/C, paclitaxel and carboplatin; PK, pharmacokinetic; SD, standard deviation; T_{max}, time to maximum plasma concentration; V_{ss}, distribution volume at steady state.

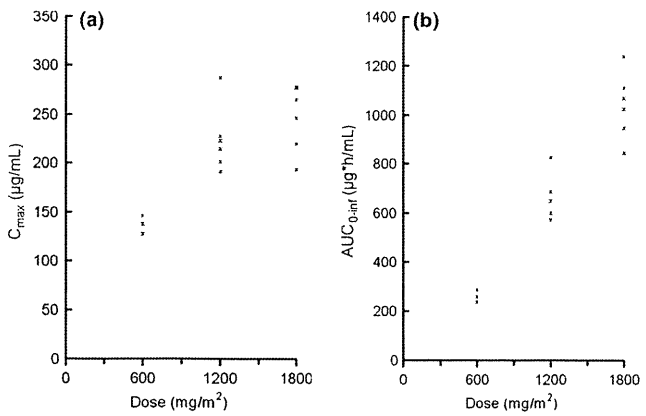

Fig. 2. Non-linear dose-exposure relationships for ASA404 at each dose level for (a) C_{max} and (b) area under the curve (AUC).

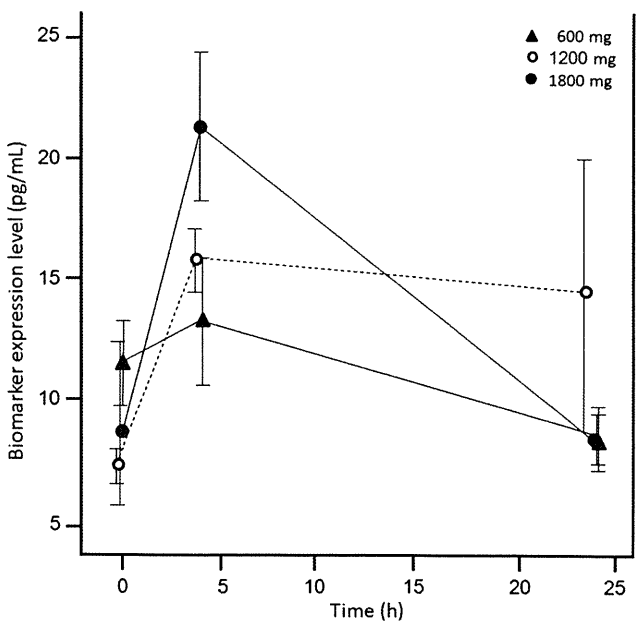

Fig. 3. Rapid dose-dependent induction of plasma 5-hydroxyindole-3-acetic acid levels after ASA404 infusion at cycle 1 day 1.

higher than baseline at 24 h post-infusion despite a post-4 h decline. Induction of 5-HIAA was dose-dependent, with increases of 116 and 204% over pre-infusion levels for 1200 and 1800 mg/m^2 dosing, respectively (Fig. 3). Induction of 5-HIAA was also observed 1 h after ASA404 infusion at all doses in cycles 2, 4 and 6. These results were in agreement with previous studies in which ASA404 caused dose-dependent acute vascular disruption and induction of plasma 5-HIAA.

Effect of ASA404 on plasma angiogenesis marker levels. No obvious changes in plasma basic fibroblast growth factor, VEGF, placental growth factor or sVEGFR-2 were observed, and sVEGFR-1 levels were highly variable.

Effect of ASA404 on plasma inflammatory cytokine and von Willebrand factor levels. On cycle 1 day1, increased plasma levels of the inflammatory cytokines interleukin-8 and monocyte chemotactic protein-1 were observed 4 and 24 h after ASA404 infusion (Fig. 4). Levels of von Willebrand factor increased 4 and 24 h after ASA404 infusion at the 1800 mg/m^2 dose, and 24 h after ASA404 infusion at the1200 mg/m^2 dose (Fig. 5).

Discussion

This single-arm, open-label study evaluated the addition of the flavonoid tumor-VDA ASA404 at three doses (600, 1200 and 1800 mg/m^2) to standard P/C therapy in 15 Japanese patients with stage IV advanced NSCLC. A total of 15 patients were treated with ASA404, and three patients (two patients at 600 mg/m^2 and one patient at 1200 mg/m^2) completed six cycles of treatment. Approximately 70% of patients received cycle three of ASA404 treatment and the median cumulative dose was similar within each dose level (6100–7600 mg). A total of 12 patients (80%) were discontinued from the study due to AEs (n = 7) or progressive disease (n = 5). All dose levels were well tolerated when administered every 3 weeks, and the incidence of DLTs was ≤1/3. This safety profile was comparable to that seen in non-Japanese patients in previous Phase I and Phase II studies.[29–33] The most frequently occurring AEs regardless of causality were injection site pain, peripheral sensory neuropathy, alopecia and neutropenia. Cardiac events were not evident in this study with the exception of QT prolongation, which, although reported in three patients, did not require therapeutic intervention and could be managed through study drug discontinuation alone. No new ophthalmological abnormalities were observed in the Japanese patients in this study, suggesting

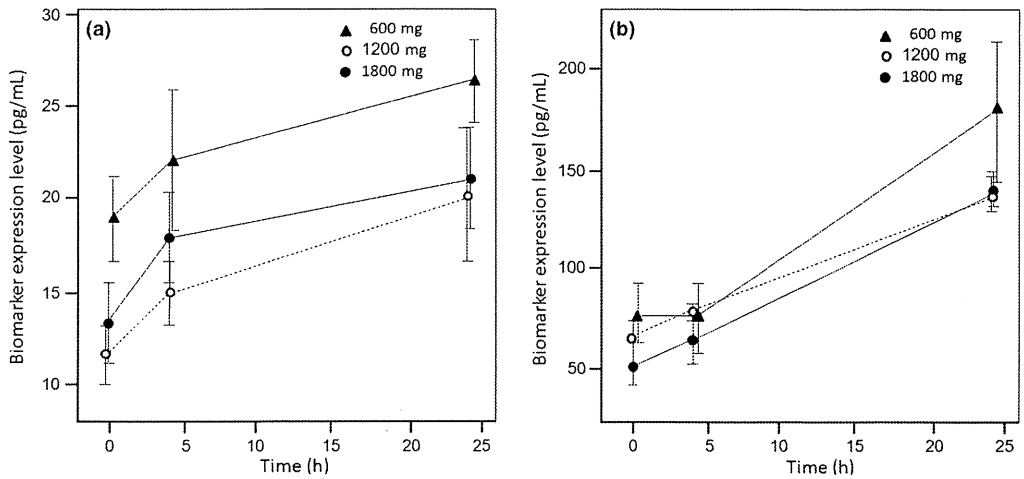

Fig. 4. Effect of ASA404 on levels of plasma inflammatory cytokines, (a) interleukin-8 and (b) monocyte chemotactic protein-1.

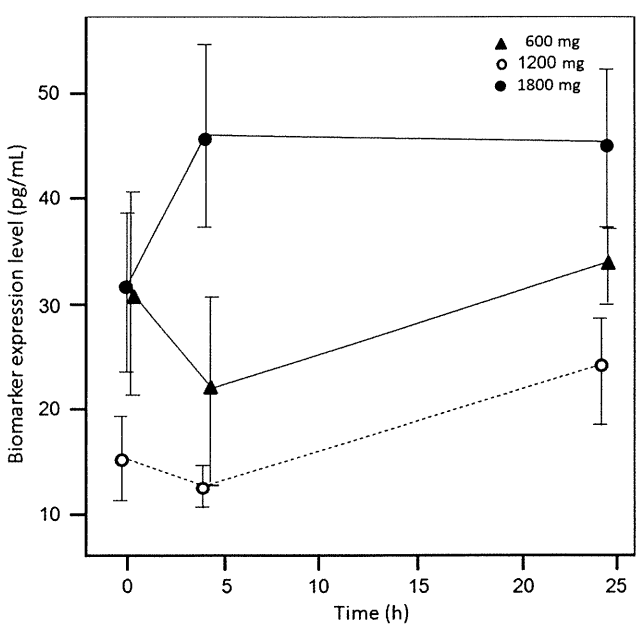

Fig. 5. Effect of ASA404 on plasma von Willebrand factor levels.

that ASA404 at dose levels up to 1800 mg/m^2 can be combined with P/C in this population without the ophthalmic AEs seen at higher doses in previous studies in non-Japanese patients.

PK data indicated saturation of systemic clearance as well as protein binding over the dose range investigated and was consistent with observations in non-Japanese patients.[30] Plasma half-life was consistent with previous studies and confirmed the observed non-accumulation following repeated dosing schedules. PD studies revealed that the pattern of changes seen in plasma angiogenesis markers after ASA404 infusion were markedly different from that seen with anti-angiogenic compounds, for which the typical response is an acute plasma VEGF and placental growth factor increase and sVEGFR-2 decrease.[36,37] The current study indicates that ASA404 has a distinctly different mechanism of action from anti-angiogenic agents with regard to these growth factors. In addition, acute induction of the inflammatory cytokines interleukin-8 and monocyte chemotactic protein-1 was observed after ASA404 infusion. This is in agreement with previous findings that ASA404 may indirectly lead to induction of inflammatory cytokines, vascular damage, and the release of von Willebrand factor.

Although the study was limited to 15 patients, tumor responses were noted, and combined with the observed safety profile, the results support the further evaluation of ASA404 at a dose of 1800 mg/m^2 in Phase III studies in combination with P/C in Japanese patients with advanced NSCLC.

Acknowledgment

Writing assistance was provided by Articulate Science, London, UK, supported by Novartis Pharmaceutical Corporation.

Disclosure Statement

Hiromi Tanii is an employee of Novartis. Michael M. Shi is an employee of Novartis, holds stocks in Novartis and receives Research funding. Ken Kobayashi is an employee of Novartis and holds stocks in Novartis.

References

1 Ferlay J. Estimates of the cancer incidence and mortality in Europe in 2006. *Ann Oncol* 2007; **18**: 581–92.
2 Parkin DM, Bray F, Ferlay J *et al.* Global cancer statistics, 2002. *CA Cancer J Clin* 2005; **55**: 74–108.
3 Govindan R. Changing epidemiology of small-cell lung cancer in the United States over the last 30 years: analysis of the Surveillance, Epidemiologic, and End Results Database. *J Clin Oncol* 2006; **24**: 4539–43.
4 Subramanian J, Govindan R. Lung Cancer. In: Govindan R, ed. *The Washington Manual of Oncology*. Philadelphia: Lippincott Williams and Wilkins, 2008; 141.
5 Shibuya K. Global and regional estimates of cancer mortality and incidence by site: II. results for the global burden of disease 2000. *BMC Cancer* 2002; **2**: 1–26.
6 Oshima A, Kuroishi T, Tajima K. *Trends of incidence rates of cancer in Japan. White Book of Cancer Statistics: Incidence Death and Prognosis*. Tokyo: Shinohara-shinsha, 2005.
7 Toyoda Y, Nakayama T, Ioka A *et al.* Trends in lung cancer incidence by histological type in Osaka, Japan. *Jpn J Clin Oncol* 2008; **38**: 534–9.
8 Vansteenkiste J, Koester M, Lange M *et al.* First-line treatment patterns in advanced NSCLC in western Europe (EU), the United States, and Japan including a comparative analysis of younger versus elderly patients. *J Clin Oncol* 2009; **27**: (15 Suppl.): 8053 [abstract].
9 NCCN. *Clinical Practice Guidelines in Oncology, v2*. NCCN, INC., 2009.

doi: 10.1111/j.1349-7006.2010.01839.x

10 NSCLC Meta-Analyses Collaborative Group. Chemotherapy in addition to supportive care improves survival in advanced non-small-cell lung cancer: a systematic review and meta-analysis of individual patient data from 16 randomized controlled trials. *J Clin Oncol* 2008; **26**: 4617–25.
11 Folkman J. What is the evidence that tumors are angiogenesis dependent? *J Natl Cancer Inst* 1990; **82**: 4–6.
12 Ushijima C, Tsukamoto S, Yamazaki K *et al.* High vascularity in the peripheral region of non-small cell lung cancer tissue is associated with tumor progression. *Lung Cancer* 2001; **34**: 233–41.
13 Cox G, Walker RA, Andi A *et al.* Prognostic significance of platelet and microvessel counts in operable non-small cell lung cancer. *Lung Cancer* 2000; **29**: 169–77.
14 Fontanini G, Lucci M, Vignati S *et al.* Angiogenesis as a prognostic indicator of survival in non-small cell lung cancer: a prospective study. *J Natl Cancer Inst* 1997; **89**: 881–6.
15 Meert A-P, Paesmans M, Martin B *et al.* The role of microvessel density on the survival of patients with lung cancer: a systematic review of the literature and meta-analysis. *Br J Cancer* 2002; **87**: 694–701.
16 Konerding MA, Miodonski AJ, Lametschwandtner A. Microvascular corrosion casting in the study of tumor vascularity: a review. *Scanning Microsc* 1995; **9**: 1233–43.
17 Tozer GM, Kanthou C, Baguley BC. Disrupting tumour blood vessels. *Nat Rev Cancer* 2005; **5**: 423–35.
18 Ching LM, Cao Z, Kieda C *et al.* Induction of endothelial cell apoptosis by the antivascular agent 5,6-dimethylxanthenone-4-acetic acid. *Br J Cancer* 2002; **86**: 1937–42.
19 Baguley BC, Ching LM. DMXAA: an antivascular agent with multiple host responses. *Int J Radiat Oncol Biol Phys* 2002; **54**: 1503–11.
20 Ching LM, Goldsmith D, Joseph WR *et al.* Induction of intratumoral tumor necrosis factor (TNF) synthesis and hemorrhagic necrosis by 5,6-dimethylxanthenone-4-acetic acid (DMXAA) in TNF knockout mice. *Cancer Res* 1999; **59**: 3304–7.
21 Ching LM, Zwain S, Baguley BC. Relationship between tumour endothelial cell apoptosis and tumour blood flow shutdown following treatment with the antivascular agent DMXAA in mice. *Br J Cancer* 2004; **90**: 906–10.
22 Zwi L, Baguley B, Gavin J *et al.* Correlation between immune and vascular activities of xanthenone acetic acid antitumor agents. *Oncol Res* 1994; **6**: 79–85.
23 McPhail LD, McIntyre DJ, Ludwig C *et al.* Rat tumor response to the vascular-disrupting agent 5,6-dimethylxanthenone-4-acetic acid as measured by dynamic contrast-enhanced magnetic resonance imaging, plasma 5-hydroxyindoleacetic acid levels, and tumor necrosis. *Neoplasia* 2006; **8**: 199–206.
24 Baguley BC, Wilson WR. Potential of DMXAA combination therapy for solid tumors. *Expert Rev Anticancer Ther* 2002; **2**: 593–603.
25 Kelland LR. Targeting established tumour vasculature: a novel approach to cancer treatment. *Curr Cancer Ther Rev* 2005; **1**: 1–9.
26 Siemann DW, Mercer E, Lepler S *et al.* Vascular targeting agents enhance chemotherapeutic agent activities in solid tumor therapy. *Int J Cancer* 2002; **99**: 1–6.
27 Siim BG, Lee AE, Shalal-Zwain S *et al.* Marked potentiation of the antitumour activity of chemotherapeutic drugs by the antivascular agent 5,6-dimethylxanthenone-4-acetic acid (DMXAA). *Cancer Chemother Pharmacol* 2003; **51**: 43–52.
28 Green C, Griffiths-Johnson D, Dunmore K. Marked potentiation of the *in vivo* antitumor activity of docetaxel in a human prostate cancer xenograft by the vascular targeting agent 5,6 dimethylxanthenone acetic acid, DMXAA. *Proc Amer Assoc Cancer Res* 2005; 2990. [abstract].
29 Jameson MB, Thompson PI, Baguley BC *et al.* Clinical aspects of a phase I trial of 5,6-dimethylxanthenone-4-acetic acid (DMXAA), a novel antivascular agent. *Br J Cancer* 2003; **88**: 1844–50.
30 McKeage MJ, Fong P, Jeffery M *et al.* 5,6-Dimethylxanthenone-4-acetic acid in the treatment of refractory tumors: a phase I safety study of a vascular disrupting agent. *Clin Cancer Res* 2006; **12**: 1776–84.
31 Rustin GJ, Bradley C, Galbraith S *et al.* 5,6-dimethylxanthenone-4-acetic acid (DMXAA), a novel antivascular agent: phase I clinical and pharmacokinetic study. *Br J Cancer* 2003; **88**: 1160–7.
32 McKeage MJ, von Pawel J, Reck M *et al.* Randomised phase II study of ASA404 combined with carboplatin and paclitaxel in previously untreated advanced non-small cell lung cancer. *Br J Cancer* 2008; **99**: 2006–12.
33 McKeage MJ, Reck M, Jameson MB *et al.* Phase II study of ASA404 (vadimezan, 5,6-dimethylxanthenone-4-acetic acid/DMXAA) 1800 mg/m^2 combined with carboplatin and paclitaxel in previously untreated advanced non-small cell lung cancer. *Lung Cancer* 2009; **65**: 192–7.
34 McKeage MJ, Jameson MB, AS1404-201 Study Group Investigators. Comparison of safety and efficacy between squamous and non-squamous non-small cell lung cancer (NSCLC) patients in phase II studies of DMXAA (ASA404). ASCO Annual Meeting. Chicago: 2008; 8072 [abstract].
35 Novartis Pharmaceuticals. NCT00662597: a Phase III, randomized, double-blind, placebo-controlled multi-center study of ASA404 in combination with paclitaxel and carboplatin as first-line treatment for locally advanced or metastatic (stage IIIb/IV) non-small cell lung cancer (NSCLC). ATTRACT-1 [cited 4 October 2010], and Available from URL: http://clinicaltrials.gov/ct2/show/NCT00662597?term=ASA404+NSCLC&rank=3
36 DePrimo S, Bello C, Smeraglia J *et al.* Circulating protein biomarkers of pharmacodynamic activity of sunitinib in patients with metastatic renal cell carcinoma: modulation of VEGF and VEGF-related proteins. *J Transl Med* 2007; **5**: 1–11.
37 Rini B, Michaelson M, Rosenberg J *et al.* Antitumor activity and biomarker analysis of sunitinib in patients with bevacizumab-refractory metastatic renal cell carcinoma. *J Clin Oncol* 2008; **26**: 3743–8.

Published OnlineFirst March 17, 2011; DOI:10.1158/1078-0432.CCR-10-2798

Clinical Cancer Research

Role of ERK-BIM and STAT3-Survivin Signaling Pathways in ALK Inhibitor–Induced Apoptosis in EML4-ALK–Positive Lung Cancer

Ken Takezawa[1], Isamu Okamoto[1], Kazuto Nishio[2], Pasi A. Jänne[3], and Kazuhiko Nakagawa[1]

Abstract

Purpose: *EML4-ALK* (echinoderm microtubule-associated protein–like 4 anaplastic lymphoma kinase) was recently identified as a transforming fusion gene in non–small cell lung cancer. The purpose of the present study was to characterize the mechanism of malignant transformation by EML4-ALK.

Experimental Design: We established NIH 3T3 cells that stably express variant 1 or 3 of EML4-ALK and examined the signaling molecules that function downstream of EML4-ALK.

Results: Forced expression of EML4-ALK induced marked activation of extracellular signal–regulated kinase (ERK) and STAT3, but not that of AKT. Inhibition of ERK or STAT3 signaling resulted in substantial attenuation of the proliferation of cells expressing either variant of EML4-ALK, suggesting that these signaling pathways function downstream of EML4-ALK in lung cancer cells. The specific ALK inhibitor TAE684 induced apoptosis that was accompanied both by upregulation of BIM, a proapoptotic member of the Bcl-2 family, and by downregulation of survivin, a member of the inhibitor of apoptosis protein (IAP) family, in EML4-ALK–expressing NIH 3T3 cells as well as in H3122 human lung cancer cells harboring endogenous EML4-ALK. Depletion of BIM and overexpression of survivin each inhibited TAE684-induced apoptosis, suggesting that both upregulation of BIM and downregulation of survivin contribute to TAE684-induced apoptosis in EML4-ALK–positive lung cancer cells. Furthermore, BIM and survivin expression was found to be independently regulated by ERK and STAT3 signaling pathways, respectively.

Conclusions: ALK inhibitor–induced apoptosis is mediated both by BIM upregulation resulting from inhibition of ERK signaling as well as by survivin downregulation resulting from inhibition of STAT3 signaling in EML4-ALK–positive lung cancer cells. *Clin Cancer Res; 17(8); 2140–8. ©2011 AACR.*

Introduction

Lung cancer is the leading cause of cancer deaths worldwide. Given that the efficacy of conventional chemotherapeutic agents with regard to improving clinical outcome in lung cancer patients is limited, target-based therapies are being pursued as potential treatment alternatives. Somatic mutations in the tyrosine kinase domain of the epidermal growth factor receptor (EGFR) have been associated with tumor responsiveness to EGFR tyrosine kinase inhibitors (TKI) in a subset of individuals with non–small cell lung cancer (NSCLC; refs. 1–3). Such findings suggest that the use of molecularly targeted therapy in genetically defined subsets of cancer patients may prove to be an effective strategy for the treatment of many cancers including NSCLC. Given that lung cancer is a common type of cancer, the identification of even small subsets of lung cancer patients harboring specific genetic abnormalities will translate into the provision of large cohorts for targeted therapy.

A recent study identified a potential driver mutation in NSCLC: fusion of the echinoderm microtubule-associated protein–like 4 gene (*EML4*) with the anaplastic lymphoma kinase gene (*ALK*), which results in the production of a fusion protein (EML4-ALK) consisting of the NH_2-terminal portion of EML4 and the COOH-terminal region of ALK (4). ALK was originally discovered as the result of characterization of chromosomal translocations that lead to the expression of fusion proteins consisting of the COOH-terminal kinase domain of ALK and the NH_2-terminal portion of nucleophosmin (NPM) in patients with anaplastic large cell lymphoma (5, 6). Various break and fusion points within the *EML4* locus in NSCLC cells give rise to different isoforms of EML4-ALK, which appear to be present in 5% to 10% of NSCLC cases (4, 7–14). The most common EML4-ALK variants are 1 and 3, which together account for about 60% of EML4-ALK–positive lung cancer cases (14). All EML4-ALK isoforms undergo constitutive oligomerization mediated by the coiled coil domain of the

Authors' Affiliations: Departments of [1]Medical Oncology and [2]Genome Biology, Kinki University Faculty of Medicine, Osaka, Japan; and [3]Lowe Center for Thoracic Oncology and Department of Medical Oncology, Dana-Farber Cancer Institute, Boston, Massachusetts

Note: Supplementary data for this article are available at Clinical Cancer Research Online (http://clincancerres.aacrjournals.org/).

Corresponding Author: Isamu Okamoto, Department of Medical Oncology, Kinki University Faculty of Medicine, 377-2 Ohno-higashi, Osaka-Sayama, Osaka 589-8511, Japan. Phone: 81-72-366-0221; Fax: 81-72-360-5000; E-mail: chi-okamoto@dotd.med.kindai.ac.jp

doi: 10.1158/1078-0432.CCR-10-2798

Published OnlineFirst March 17, 2011; DOI:10.1158/1078-0432.CCR-10-2798

Translational Relevance

EML4-ALK (echinoderm microtubule-associated protein–like 4 anaplastic lymphoma kinase) was recently identified as a transforming fusion gene in non–small cell lung cancer (NSCLC), and several selective inhibitors of the kinase activity of ALK, such as crizotinib, are currently undergoing clinical trials for the treatment of EML4-ALK–positive NSCLC. Identification of the signaling pathways responsible for malignant transformation by EML4-ALK will likely enhance further development of ALK-targeted therapy for NSCLC patients. We have now shown that both ERK (extracellular signal–regulated kinase) and STAT3 pathways are the principal mediators of EML4-ALK signaling, and we further identified the mediators of apoptosis induced by ALK inhibition. Our preclinical data provide both insight into the pathogenesis of EML4-ALK–positive lung cancer and a potential basis for the development of biomarkers for the efficacy of ALK-targeted therapy in patients with this condition.

EML4 portion, which confers marked transforming activity both *in vitro* and *in vivo* (4, 15).

ALK inhibitors have been found to suppress the growth of and to induce apoptosis in EML4-ALK–positive lung cancer cells, suggesting that ALK inhibition is a potential strategy for the treatment of NSCLC patients with this molecular abnormality (9, 16). Indeed, a selective inhibitor of the kinase activity of ALK, crizotinib, is currently undergoing clinical trials and has shown high efficacy in NSCLC patients with EML4-ALK (17). However, the downstream signaling pathways that regulate the proliferation or survival of EML4-ALK–positive lung cancer cells have remained to be well established, and the key mediators of ALK inhibitor–induced apoptosis have not been fully determined. In the present study, we constructed expression vectors for EML4-ALK variants 1 and 3 and then established cells stably expressing these proteins. With the use of these cells, we examined the signaling molecules that function downstream of EML4-ALK. We further investigated the molecular mechanisms underlying ALK inhibitor–induced apoptosis in EML4-ALK–positive lung cancer cells.

Materials and Methods

Cell culture and reagents

NIH 3T3 cells as well as the human cancer cell lines H2228 and Karpas299 were obtained from American Type Culture Collection. H3122 cells were obtained as previously described (9). NIH 3T3 cells were cultured in Dulbecco's modified Eagle's medium (Sigma) supplemented with 10% FBS and 1% penicillin-streptomycin. H2228, Karpas299, and H3122 cells were cultured in RPMI 1640 medium (Sigma) supplemented with 10% FBS and 1% penicillin-streptomycin. All cells were maintained under a humidified atmosphere of 5% CO_2 at 37°C. U0126 and LY294002 were obtained from Cell Signaling Technology and TAE684 was from ShangHai Biochempartner.

Cell transfection

A cDNA for EML4-ALK variant 1 was cloned into pDNR-Dual (Becton Dickinson) as previously described (9). A full-length cDNA fragment encoding EML4-ALK variant 3b was obtained from H2228 cells by reverse transcription and the PCR with the primers EAV-F (5′-AAGCTTCGCAAGATGGACGGTTTCGCCGGCAGTC-3′) and EAV-R (5′-GCGGCCGCTCAGGGCCCAGGC-TGGTTCATGCT-3′). Amplification products were verified by sequencing after their cloning into the pCR-Blunt II-TOPO vector (Invitrogen). The EML4-ALK variant 1 or 3b cDNA was excised from pCR-Blunt II-TOPO and transferred to either pcDNA3.1-Hygro(+) (Invitrogen) or pMZs (Cell Biolabs). A pBabe-puro vector encoding CA-STAT3 with a COOH-terminal FLAG tag was kindly provided by J. Bromberg (18). A pQCXIH-survivin vector was constructed as previously described (19). All expression vectors were introduced into NIH 3T3 cells as previously described (20, 21).

Immunoblot analysis

Cells were washed twice with ice-cold PBS and then lysed in a solution containing 20 mmol/L Tris-HCl (pH 7.5), 150 mmol/L NaCl, 1 mmol/L EDTA, 1% Triton X-100, 2.5 mmol/L sodium pyrophosphate, 1 mmol/L phenylmethylsulfonyl fluoride, and leupeptin (1 μg/mL). The protein concentration of cell lysates was determined with the Bradford reagent (Bio-Rad), and equal amounts of protein were subjected to SDS-PAGE on a 7.5% or 12% gel. The separated proteins were transferred to a nitrocellulose membrane, which was then exposed to 5% nonfat dried milk in PBS for 1 hour at room temperature before incubation overnight at 4°C with primary antibodies. Rabbit polyclonal antibodies to human phosphorylated ALK (pY1608), to ALK, to phosphorylated extracellular signal–regulated kinase (ERK), to ERK, to phosphorylated STAT3, to STAT3, to phosphorylated AKT, to AKT, to PARP, to BIM, to Mcl-1, to Bcl-xL, to X-linked inhibitor of apoptosis (XIAP), and to FLAG were obtained from Cell Signaling Technology; those to survivin were from Novos; and those to β-actin were from Sigma. All antibodies were used at a 1:1,000 dilution, with the exception of those to β-actin (1:200). The membrane was then washed with PBS containing 0.05% Tween 20 before incubation for 1 hour at room temperature with horseradish peroxidase–conjugated goat antibodies to rabbit IgG (Sigma). Immune complexes were finally detected with chemiluminescence reagents (GE Healthcare).

Cell growth inhibition assay

Cells were plated in 96-well, flat-bottomed plates and cultured for 24 hours before exposure to various concentrations of drugs for 72 hours. TetraColor One (5 mmol/L tetrazolium monosodium salt and 0.2 mmol/L 1-methoxy-5-methyl phenazinium methylsulfate; Seikagaku) was then

Published OnlineFirst March 17, 2011; DOI:10.1158/1078-0432.CCR-10-2798

added to each well, and the cells were incubated for 3 hours at 37°C before measurement of absorbance at 490 nm with a Multiskan Spectrum instrument (Thermo Labsystems).

RNA interference

Cells were plated at 50% to 60% confluence in 6-well plates or 25-cm^2 flasks and then incubated for 24 hours before transient transfection for the indicated times with siRNAs mixed with the Lipofectamine reagent (Invitrogen). The siRNAs specific for STAT3 mRNA (STAT3-1, 5′-UCAUUGACCUUGUGAAAAA-3′; STAT3-2, 5′-GCAAAAA-GUUUCCUACAAA-3′), ALK mRNA (ALK-1, 5′-ACACC-CAAAUUAAUACCAA-3′; ALK-2, 5′-UCAGCAAAUUCAA-CCACCA-3′), ERK mRNA (ERK-1, 5′-CAAGAGGAUUGAA-GUAGAA-3′; ERK-2, 5′-UCAGCCCCUUUGAGCACCA-3′), or BIM mRNA (BIM-1, 5′-GGAGGGUAUUUUUGAAUAA-3′; BIM-2, 5′-AGGAGGGUAUUUUUGAAUA-3′) as well as a nonspecific siRNA (5′-GUUGAGAGAUAUUAGAGUU-3′) were obtained from Nippon EGT. The cells were then subjected to immunoblot analysis or the annexin V–binding assay. All data presented were obtained with STAT3-1, ALK-1, ERK-1, or BIM-1 siRNAs, but similar results were obtained with STAT3-2, ALK-2, ERK-2, and BIM-2 siRNAs.

Annexin V–binding assay

Binding of annexin V to cells was measured with the use of an Annexin-V-FLUOS Staining kit (Roche). Cells were harvested by exposure to trypsin-EDTA, washed with PBS, and centrifuged at 200 × *g* for 5 minutes. The cell pellets were resuspended in 100 μL of Annexin-V-FLUOS labeling solution, incubated for 10 to 15 minutes at 15°C to 25°C, and then analyzed for fluorescence with a flow cytometer (FACSCalibur) and Cell Quest software (Becton Dickinson).

Statistical analysis

Quantitative data are presented as means ± SD and were analyzed by Student's 2-tailed *t* test. A value of $P < 0.05$ was considered statistically significant.

Results

Oncogenic EML4-ALK tyrosine kinase activates ERK and STAT3 signaling pathways

To study the function of oncogenic EML4-ALK, we established nontransformed mouse fibroblast (NIH 3T3) cells that either stably express EML4-ALK variant 1 or 3 (3T3/EAV1 and 3T3/EAV3 cells, respectively) or stably harbor the corresponding empty vector (3T3-Mock cells). Immunoblot analysis revealed that EML4-ALK variant 1 or 3 was detected with antibodies to ALK at positions corresponding to molecular sizes of about 120 and 90 kDa, respectively, in the transfected cells (Fig. 1A). The kinase activity of the EML4-ALK variants was activated as revealed by immunoblot

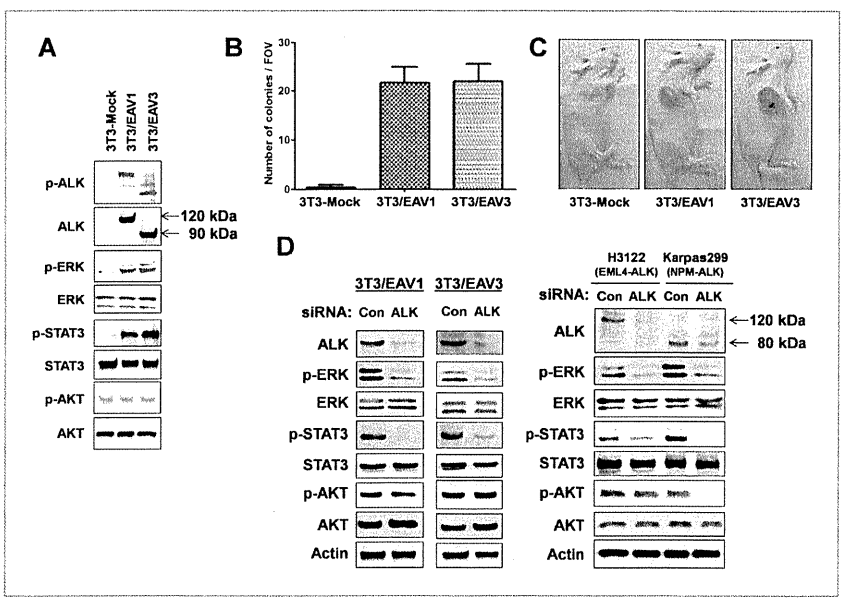

Figure 1. Effects of stable forced expression of EML4-ALK variant 1 or 3 on signaling pathways. A, the indicated stably transfected NIH 3T3 cell lines were lysed and subjected to immunoblot analysis with antibodies to the indicated proteins. B, the indicated cell lines were plated in semisolid medium supplemented with 10% FBS and incubated for 3 to 4 weeks, after which the cells were stained with 0.005% crystal violet and the number of colonies per field of view (FOV) was counted. Data are means ± SD from 3 independent experiments. C, cells (5×10^6) of the indicated lines were injected subcutaneously into the axilla of 5-week-old female athymic nude mice. At 18 days after the injection, the large tumors that formed at the injection site for 3T3/EAV1 or 3T3/EAV3 cells were photographed. Data are representative of results obtained with 5 mice per cell line. D, the indicated cell lines were transfected with nonspecific (Con) or ALK siRNAs for 48 hours, after which cell lysates were subjected to immunoblot analysis with antibodies to the indicated proteins.

Published OnlineFirst March 17, 2011; DOI:10.1158/1078-0432.CCR-10-2798

analysis with antibodies specific for the Tyr^{1608}-phosphorylated form of ALK. Consistent with previous observations (4, 15), the 3T3/EAV cells exhibited transforming activity both *in vitro* (Fig. 1B) and *in vivo* (Fig. 1C). We also found that phosphorylation of both the mitogen-activated protein kinase (MAPK) ERK and STAT3 was markedly increased in the cells expressing either variant of EML4-ALK compared with that in 3T3-Mock cells, whereas the phosphorylation level of the kinase AKT was not affected by expression of EML4-ALK (Fig. 1A). To exclude the possibility that these results were due to nonspecific effects of transfection, we depleted both 3T3/EAV1 and 3T3/EAV3 cells of EML4-ALK by RNA interference (RNAi) with ALK siRNA. The phosphorylation of both ERK and STAT3, but not that of AKT, was markedly suppressed by depletion of EML4-ALK (Fig. 1D). Moreover, similar depletion of endogenous EML4-ALK variant 1 in the lung cancer cell line H3122 resulted in marked inhibition of the phosphorylation of ERK and STAT3 without an effect on that of AKT (Fig. 1D). In contrast, the phosphorylation of ERK, STAT3, and AKT was inhibited by ALK siRNA in the NPM-ALK–positive lymphoma cell line Karpas299 (Fig. 1D), in which activation of the phosphoinositide 3-kinase (PI3K)-AKT signaling pathway has been shown to contribute to malignant transformation (22–25). Together, these data suggested that either variant 1 or 3 of EML4-ALK activates ERK and STAT3 signaling pathways but not the PI3K-AKT signaling pathway.

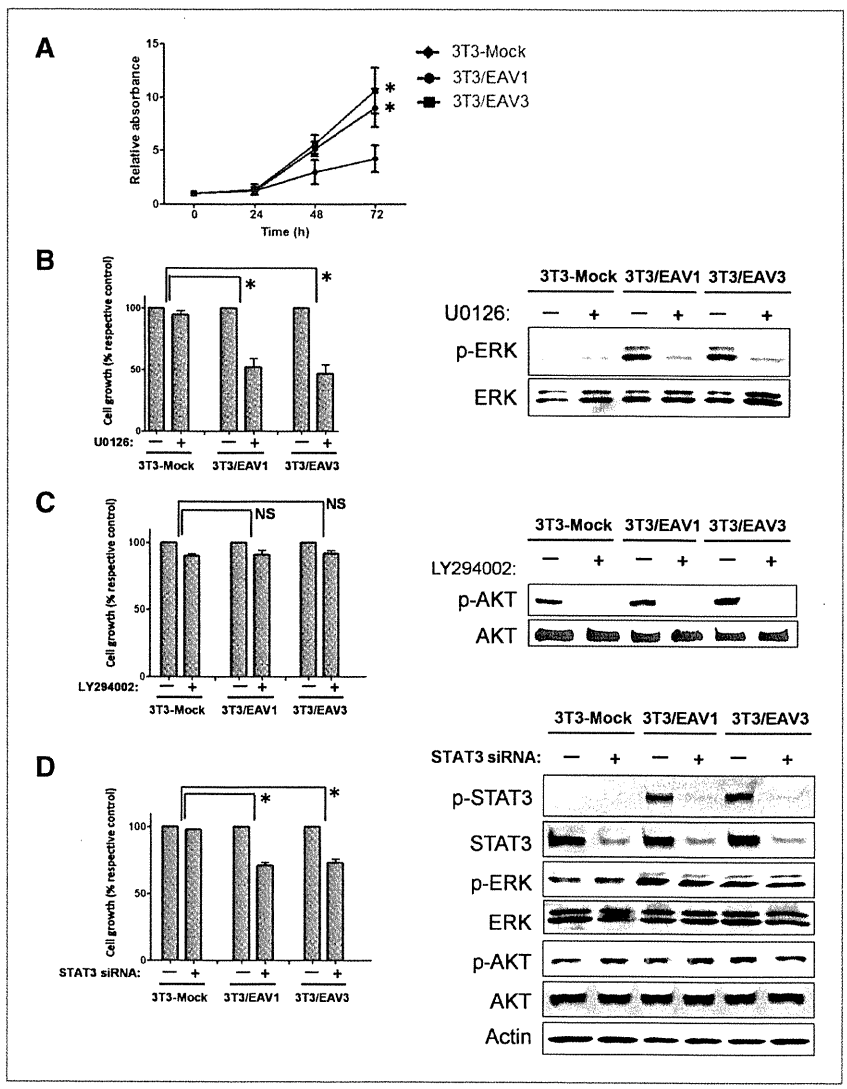

Figure 2. Effects of inhibition of ERK, PI3K, or STAT3 signaling on the growth of cells expressing EML4-ALK. A, the indicated cell lines were incubated in complete medium for the indicated times, after which cell viability was assessed as described in the "Materials and Methods" section. Data are expressed relative to the absorbance value for 3T3-Mock cells at time 0. B and C, cells were incubated in complete medium with or without 10 μmol/L U0126 (B) or 10 μmol/L LY294002 (C) for 72 or 24 hours, after which cell viability was assessed (left) or cell lysates were subjected to immunoblot analysis with antibodies to the indicated proteins (right), respectively. D, cells were transfected with nonspecific or STAT3 siRNAs for 72 or 48 hours, after which cell viability was assessed (left) or cell lysates were subjected to immunoblot analysis with antibodies to the indicated proteins (right), respectively. The abundance of β-actin was examined as a loading control. All quantitative data are means ± SD from 3 independent experiments. *, $P < 0.05$ versus the corresponding value for 3T3-Mock cells or for the indicated comparisons. NS, not significant.

Published OnlineFirst March 17, 2011; DOI:10.1158/1078-0432.CCR-10-2798

EML4-ALK promotes cell proliferation through ERK and STAT3 signaling pathways

We next examined the effect of EML4-ALK on cell proliferation. Both 3T3/EAV1 and 3T3/EAV3 cells proliferated significantly faster than did 3T3-Mock cells (Fig. 2A). To determine the role of intracellular signaling pathways in this action of EML4-ALK, we first examined the effects of chemical inhibitors. We found that U0126, an inhibitor of the ERK kinase MEK, had little effect on the growth of 3T3-Mock cells but that it significantly inhibited the proliferation of both 3T3/EAV1 and 3T3/EAV3 cells at a concentration (10 μmol/L) that resulted in marked inhibition of ERK phosphorylation (Fig. 2B). These data thus suggested that the MEK-ERK signaling pathway contributes to the regulation of cell proliferation by EML4-ALK. We also found that the specific PI3K inhibitor LY294002 had no significant effect on the growth of 3T3-Mock cells or on that of 3T3/EAV1 and 3T3/EAV3 cells at a concentration (10 μmol/L) at which the phosphorylation of AKT was largely abolished (Fig. 2C). To examine the effect of STAT3 inhibition on cell proliferation in cells expressing EML4-ALK, we transfected the cells with an siRNA specific for STAT3 mRNA. Transfection of 3T3-Mock, 3T3/EAV1, or 3T3/EAV3 cells with STAT3 siRNA resulted in marked depletion of STAT3 (Fig. 2D). Whereas such depletion of STAT3 did not affect the proliferation of 3T3-Mock cells, it significantly inhibited that of 3T3/EAV1 and 3T3/EAV3 cells (Fig. 2D). A

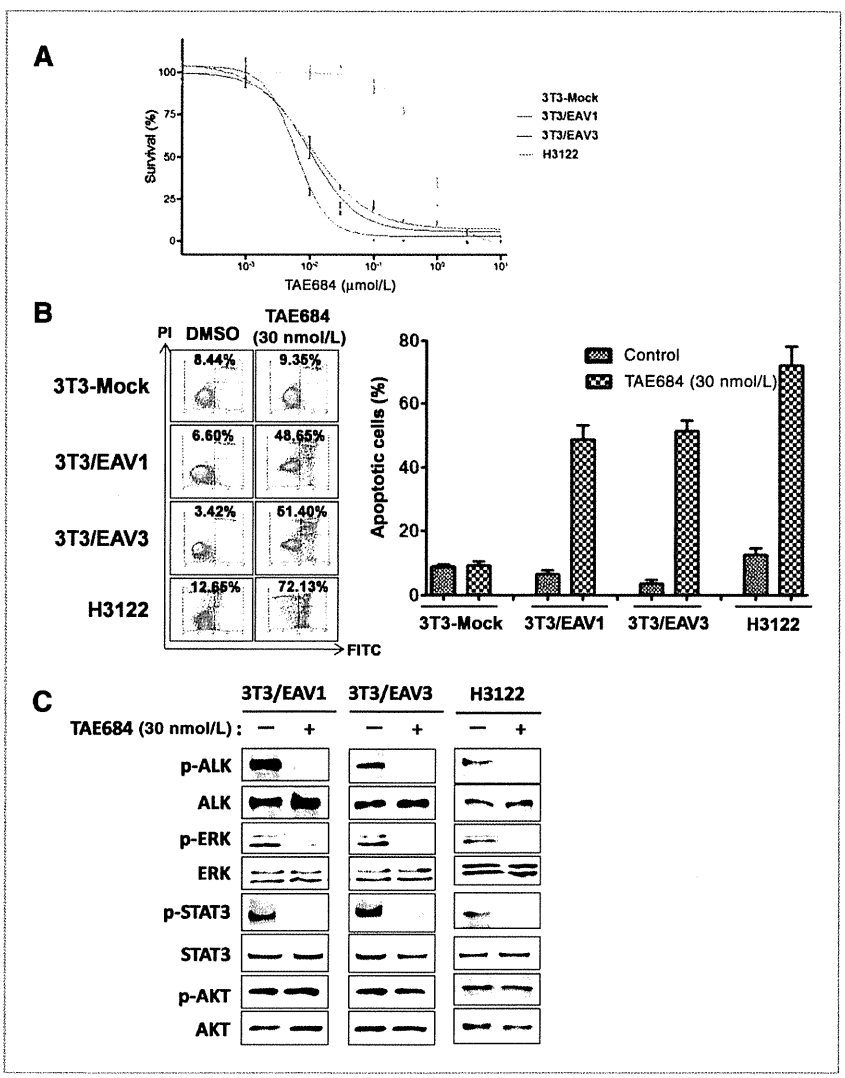

Figure 3. Effects of TAE684 on cell growth, apoptosis, and intracellular signaling in cells expressing EML4-ALK. A, the indicated cell lines were cultured for 72 hours in complete medium containing various concentrations of TAE684, after which cell viability was assessed. Data are expressed as percent survival and are means ± SD of triplicates from an experiment that was repeated a total of 3 times with similar results. B, cells were incubated for 48 hours in serum-free medium with 30 nmol/L TAE684 or 0.01% dimethyl sulfoxide (DMSO, vehicle control), after which the proportion of apoptotic cells was determined by staining with fluorescein isothiocyanate (FITC)-conjugated annexin V and propidium iodide (PI) followed by flow cytometry. Representative flow cytometric profiles, with the percentages of FITC-positive, PI-negative (apoptotic) cells indicated, are shown in the left. Quantitative data in the right are means ± SD of triplicates from an experiment that was repeated a total of 3 times with similar results. C, cells were incubated for 24 hours in serum-free medium with or without 30 nmol/L TAE684, after which cell lysates were subjected to immunoblot analysis with antibodies to the indicated proteins.

Published OnlineFirst March 17, 2011; DOI:10.1158/1078-0432.CCR-10-2798

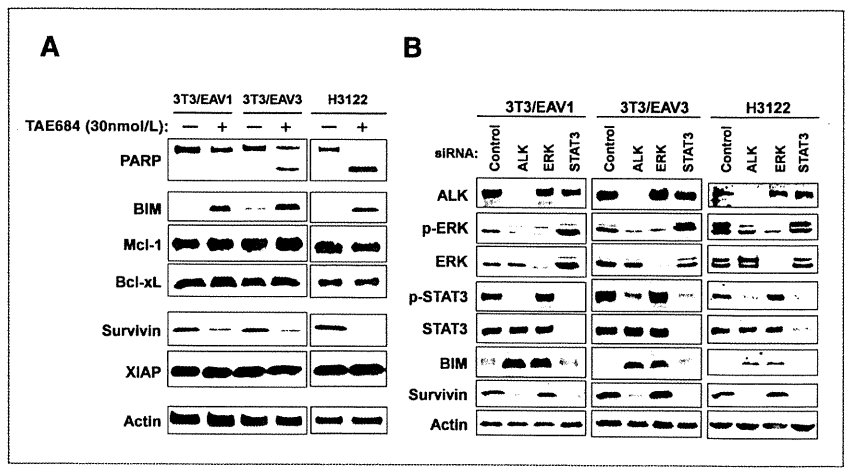

Figure 4. Effects of TAE684 on the expression of apoptosis-related proteins in cells expressing EML4-ALK. A, the indicated cell lines were incubated for 48 hours in serum-free medium with or without 30 nmol/L TAE684, after which cell lysates were subjected to immunoblot analysis with antibodies to the indicated proteins. B, 3T3/EAV1, 3T3/EAV3, or H3122 cells were transfected with nonspecific (control), ALK, ERK, or STAT3 siRNAs for 48 hours, after which cell lysates were subjected to immunoblot analysis with antibodies to the indicated proteins.

second siRNA targeted to a different region of STAT3 mRNA yielded similar results (data not shown). These observations thus suggested that EML4-ALK promotes cell proliferation through both MEK-ERK and STAT3 signaling pathways but not through the PI3K-AKT signaling pathway.

Effects of ALK inhibition on cell growth and intracellular signaling in EML4-ALK–positive lung cancer cells

To investigate the effects of inhibition of the kinase activity of ALK on cell growth and intracellular signaling in cells expressing EML4-ALK, we used TAE684, a selective and highly potent ALK inhibitor (26). The human lung cancer cell line H3122 expresses endogenous EML4-ALK variant 1 and its growth was found to be highly sensitive to TAE684 (Fig. 3A). Treatment with TAE684 also induced a large increase in the number of apoptotic H3122 cells, as revealed with an annexin V–binding assay (Fig. 3B). Consistent with these results, both 3T3/EAV1 and 3T3/EAV3 cells exhibited a sensitivity to TAE684 that was about 100 times as great as that of 3T3-Mock cells (Fig. 3A), and the level of apoptosis induced by this drug was markedly greater in both 3T3/EAV1 and 3T3/EAV3 cells than in 3T3-Mock cells (Fig. 3B). Immunoblot analysis revealed that TAE684 inhibited the phosphorylation of EML4-ALK in 3T3/EAV1, 3T3/EAV3, and H3122 cells at a concentration (30 nmol/L) at which it substantially inhibited the growth of these cells (Fig. 3C). We further found that TAE684 inhibited the activation of ERK and STAT3, without affecting that of AKT, in all 3 of these cell lines (Fig. 3C). These data thus suggested that the ALK inhibitor induced growth suppression and apoptosis in EML4-ALK–positive lung cancer cells, and that these effects were accompanied by inhibition of ERK and STAT3 signaling pathways but not by that of the PI3K-AKT signaling pathway.

Effects of ALK inhibition on the expression of apoptosis-related proteins in EML4-ALK–positive lung cancer cells

Given that TAE684 induced apoptosis in cells expressing EML4-ALK, we examined the effects of this drug on the expression of apoptosis-related proteins in such cells. TAE684 induced cleavage of PARP, a characteristic of apoptosis, in H3122 cells as well as in 3T3/EAV1 and 3T3/EAV3 cells (Fig. 4A). TAE684 also increased the abundance of BIM, a proapoptotic member of the Bcl-2 family of proteins, in cells expressing EML4-ALK, whereas the amounts of the Bcl-2 family members Mcl-1 and Bcl-xL remained unaffected (Fig. 4A). In contrast, TAE684 induced downregulation of the expression of survivin, a member of the IAP family, in cells expressing EML4-ALK, whereas the expression of XIAP, another IAP family member, remained unaffected (Fig. 4A). To investigate the possible roles of the ERK and STAT3 signaling pathways in the induction of BIM and downregulation of survivin by TAE684, we examined the effects of EML4-ALK, ERK, or STAT3 depletion by RNAi in 3T3/EAV1, 3T3/EAV3, and H3122 cells. Similar to the effects of TAE684 (Fig. 3C), depletion of EML4-ALK with an ALK siRNA resulted in inhibition of both ERK and STAT3 phosphorylation in all 3 cell lines (Fig. 4B). The amount of BIM was increased as a result of EML4-ALK or ERK depletion but was not affected by STAT3 depletion (Fig. 4B). In contrast, the expression of survivin was inhibited by depletion of EML4-AKT or STAT3 but not by that of ERK (Fig. 4B). Similar results were obtained with a second set of ALK, ERK, and STAT3 siRNAs targeted to different regions of the corresponding mRNAs (data not shown). These data thus suggested that ALK inhibition results in upregulation of BIM expression through inhibition of the ERK signaling pathway as well as in downregulation of survivin expression through inhibition of the STAT3 signaling pathway.

Published OnlineFirst March 17, 2011; DOI:10.1158/1078-0432.CCR-10-2798

Role of ERK-BIM and STAT3-survivin signaling pathways in TAE684-induced apoptosis in cells expressing EML4-ALK

To investigate further whether induction of BIM is related to TAE684-induced apoptosis, we transfected 3T3/EAV3 or H3122 cells with an siRNA specific for BIM mRNA. Such transfection largely blocked BIM induction by TAE684 (Fig. 5A). Staining with annexin V revealed that RNAi-mediated attenuation of BIM induction resulted in significant inhibition of TAE684-induced apoptosis in both cell lines (Fig. 5A), implicating upregulation of BIM expression in the induction of apoptosis by TAE684 in EML4-ALK–positive cells. We obtained similar results with a second siRNA targeted to a different sequence within BIM mRNA (data not shown). Given that TAE684 inhibited STAT3-survivin signaling in cells expressing EML4-ALK, we next investigated the contribution of such signaling to TAE684-induced apoptosis by transfecting 3T3/EAV3 or H3122 cells with an expression vector encoding a FLAG epitope–tagged constitutively active (CA) form of human STAT3. Expression of CA-STAT3 increased the abundance of survivin (Fig. 5B), consistent with the notion that survivin expression is upregulated by activation of STAT3 signaling. Furthermore, expression of CA-STAT3 inhibited the downregulation of survivin induced by TAE684, without affecting BIM induction (Fig. 5B), and it significantly inhibited TAE684-induced apoptosis (Fig. 5B). These data suggested that inhibition of the STAT3 signaling pathway contributes to TAE684-induced apoptosis in EML4-ALK–positive cells. To confirm that TAE684-induced apoptosis mediated by STAT3 inhibition was attributable to downregulation of survivin expression, we transfected 3T3/EAV3 or H3122 cells with an expression vector for human survivin. Survivin overexpression resulted in substantial inhibition of the TAE684-induced downregulation of survivin in both 3T3/EAV3 and H3122 cells (Fig. 5C), and this effect was associated with significant inhibition

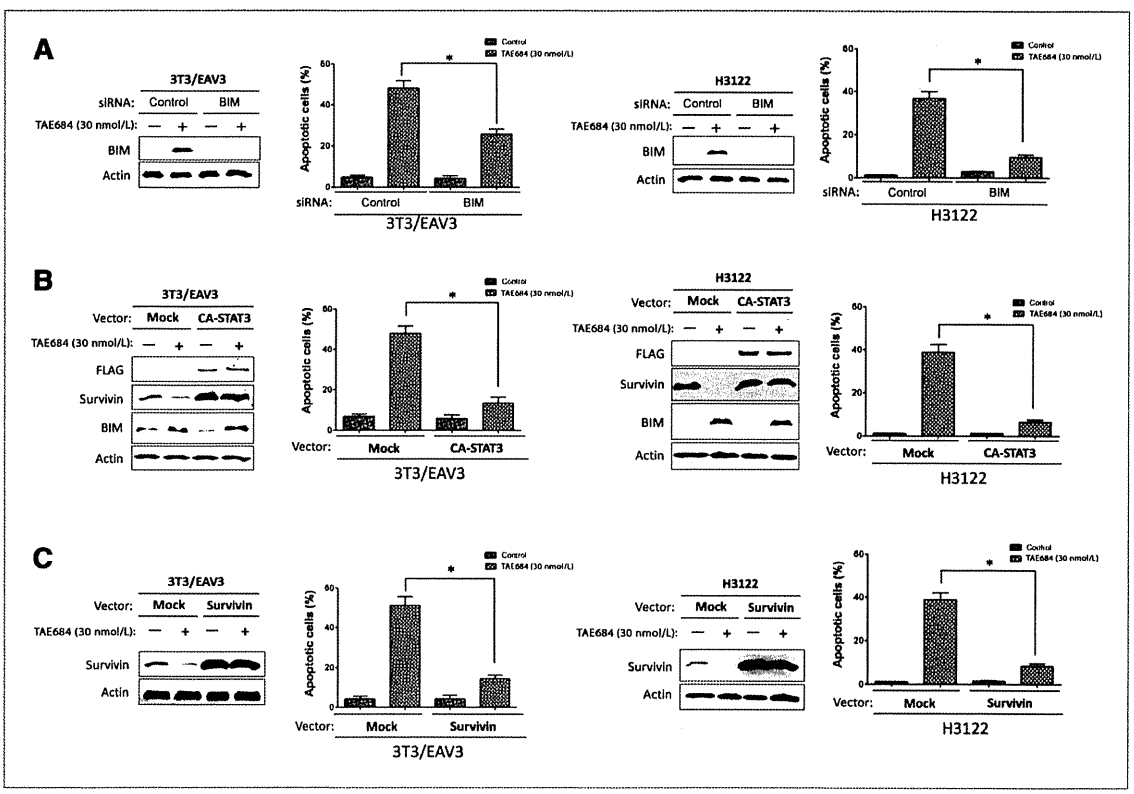

Figure 5. Effects of BIM depletion as well as forced expression of CA-STAT3 and survivin on apoptosis induced by TAE684 in 3T3/EAV3 or H3122 cells. A, cells were transfected with nonspecific (control) or BIM siRNAs for 24 hours and then incubated in complete medium with 30 nmol/L TAE684 or DMSO vehicle for 48 hours, after which cells either were lysed and subjected to immunoblot analysis with antibodies to the indicated proteins or were evaluated for apoptosis by staining with annexin V and PI followed by flow cytometry. B, cells were transfected with an expression vector for FLAG-tagged CA-STAT3 or with the corresponding empty vector for 24 hours and were then incubated with or without 30 nmol/L TAE684 for 48 hours and analyzed as in A. C, cells were transfected with an expression vector for survivin or with the corresponding empty vector for 24 hours and were then incubated with or without 30 nmol/L TAE684 for 48 hours and analyzed as in A. All quantitative data are means ± SD from at least 3 independent experiments. *, $P < 0.05$ for the indicated comparisons.